

Dear Dr. Jason Surratt,

Thank you very much for your technical suggestions on our manuscript of “acp-2018-262”. Please see the point-by-point responses below and changes are marked blue in the revised manuscript.

Thank you for considering all 4 reviewer comments. After careful re-reading of the revised manuscript, I feel you have clearly addressed these comments. However, upon reading the newest version, I found several minor edits/technical corrections that must be corrected. Once you correct these, I'll gladly accept this for final publication in ACP.

Minor Edits/Technical Corrections:

1.) *Page 1, Lines 16-17: change to: "we chemically characterized OSs and nitrooxy OSs (NOSs) formed under the influence of....."*

**Response:** Changed accordingly (line 16-17).

2.) *Page 1, Line 18: change "The" to "A ultrahigh-resolution"*

**Response:** Changed accordingly (line 18).

3.) *Page 1, Line 21: delete the word "the' before "high"*

**Response:** Revised accordingly (line 21).

4.) *Page 2, Line 42: Insert the word "the" between "in" and "ambient"*

**Response:** Revised accordingly (line 42).

5.) *Page 2, Line 49:*

*Change "Many chamber experiments studied try to reveal" to "Many prior chamber experiments revealed the precursors....."*

**Response:** Changed accordingly (line 49).

6.) *Pages 2-3, Lines 49-51: Please add Surratt et al. (2007, ES&T) to this citation.*

**Response:** The reference is now added (line 49).

7.) *Page 3, Line 51: Change ", which remain unclear" to "however, the atmospheric relevance of these remains unclear."*

**Response:** Changed accordingly (line 51).

8.) *Page 5, Line 101: Please change "environment" to "environmental"*

**Response:** Changed accordingly (line 101).

9.) *Page 5, Line 118: Should the authors consider adding ", respectively." after "..., China)" ?*

**Response:** Revised accordingly (line 118).

10.) *Page 6, Line 129: Can the authors clarify how much of the isoprene-derived OSs were not captured by your direct infusion method due to the use of SPE? I know from personal experience that when we analyzed PM<sub>2.5</sub> samples collected from the southeastern U.S. and applied SPE, we did not detect isoprene-derived OSs (Gao et al., 2016, JGR). As a result, in*

*Surratt et al. (2017, ES&T), we found that there were indeed present when using LC/MS and not employing an SPE pretreatment step.*

**Response:** Our results are consistent with your previous work (Gao et al., 2006; Surratt et al., 2007). Isoprene-derived OSs were not detected in SPE-treated samples, while they were detected in samples without undergoing the SPE pretreatment procedure. We now have added the following text to page 6 to clarify the impact of the SPE treatment on OSs detected.

Lines 132-136:

“Some selected OS species of low MW (e.g., isoprene-derived OSs such as  $C_4H_7O_7S^-$ ,  $C_5H_7O_7S^-$ , and  $C_5H_{11}O_7S^-$ ) would be removed by the SPE clean-up procedure and thus not detected by the direct infusion Orbitrap MS analysis (see section 3.1). We note that these OS species were detected by HPLC-MS in the sample extracts to which no SPE pretreatment procedure was applied (see section 2.3). This phenomenon was also reported in previous studies (Gao et al., 2006; Surratt et al., 2007).”

Most sincerely,

Min Hu and Jianzhen Yu

# The Secondary Formation of Organosulfates under the Interactions between Biogenic Emissions and Anthropogenic Pollutants in Summer of Beijing

Yujue Wang,<sup>1</sup> Min Hu,<sup>\*,1,5</sup> Song Guo,<sup>1</sup> Yuchen Wang,<sup>3</sup> Jing Zheng,<sup>1</sup> Yudong Yang,<sup>1</sup> Wenfei Zhu,<sup>6</sup> Rongzhi Tang,<sup>1</sup> Xiao Li,<sup>1</sup> Ying Liu,<sup>1,5</sup> Michael Le Breton,<sup>2</sup> Zhuofei Du,<sup>1</sup> Dongjie Shang,<sup>1</sup> Yusheng Wu,<sup>1</sup> Zhijun Wu,<sup>1</sup> Yu Song,<sup>1</sup> Shengrong Lou,<sup>6</sup> Mattias Hallquist,<sup>2</sup> and Jianzhen Yu<sup>\*,3,4</sup>

<sup>1</sup>State Key Joint Laboratory of Environmental Simulation and Pollution Control, College of Environmental Sciences and Engineering, Peking University, Beijing 100871, China

<sup>2</sup>Department of Chemistry and Molecular Biology, University of Gothenburg, Gothenburg, Sweden

<sup>3</sup>Environmental Science Programs, Hong Kong University of Science & Technology, Hong Kong, China

<sup>4</sup>Department of Chemistry, Hong Kong University of Science & Technology, Hong Kong, China

<sup>5</sup>Beijing Innovation Center for Engineering Sciences and Advanced Technology, Peking University, Beijing 100871, China

<sup>6</sup>Shanghai Academy of Environmental Sciences, Shanghai 200233, China

Correspondence to: Min Hu ([minhu@pku.edu.cn](mailto:minhu@pku.edu.cn)); Jianzhen Yu ([jian.yu@ust.hk](mailto:jian.yu@ust.hk))

**Abstract.** Organosulfates (OSs), with ambiguous formation mechanisms, are a potential source of “missing secondary organic aerosol (SOA)” in current atmospheric models. In this study, we chemically characterized OSs and nitroxy OSs (NOSs) formed under the influence of biogenic emissions and anthropogenic pollutants (e.g. NO<sub>x</sub>, SO<sub>4</sub><sup>2-</sup>) in summer of Beijing. An ultrahigh-resolution mass spectrometer equipped with electrospray ionization source was applied to examine the overall molecular composition of S-containing organics. The number and intensities of S-containing organics, the majority of which could be assigned as OSs and NOSs, increased significantly during pollution episodes, which indicated their importance for SOA accumulation. To further investigate the distribution and formation of OSs and NOSs, high performance liquid chromatography coupled to mass spectrometry was employed to quantify ten OSs and three NOS species. The total concentrations of quantified OSs and NOSs were 41.4 and 13.8 ng/m<sup>3</sup>, respectively. Glycolic acid sulfate was the most abundant species among all the quantified species, followed by monoterpene NOSs (C<sub>10</sub>H<sub>16</sub>NO<sub>7</sub>S). The total concentration of three isoprene OSs was 14.8 ng/m<sup>3</sup> and the isoprene OSs formed via HO<sub>2</sub> channel was higher than those formed via NO/NO<sub>2</sub> channel. The OS concentration coincided with the increase of acidic sulfate aerosols, aerosol acidity and liquid

27 water content (LWC), indicating the acid-catalyzed aqueous-phase formation of OSs in the presence of acidic sulfate  
28 aerosols. When sulfate dominated the accumulation of secondary inorganic aerosols (SIAs, sulfate, nitrate and ammonium)  
29 ( $\text{SO}_4^{2-}/\text{SIAs} > 0.5$ ), OS formation would be obviously promoted as the increasing of acidic sulfate aerosols, aerosol LWC and  
30 acidity ( $\text{pH} < 2.8$ ). Otherwise, the acid-catalyzed OS formation would be limited by lower aerosol acidity when nitrate  
31 dominated the SIA accumulation. The nighttime enhancement of monoterpene NOSs suggested their formation via nighttime  
32  $\text{NO}_3$ -initiated oxidation of monoterpene under high- $\text{NO}_x$  conditions. However, isoprene NOSs are supposed to form via  
33 acid-catalyzed chemistry or reactive uptake of oxidation products of isoprene. This study provides direct observational  
34 evidence and highlights the secondary formation of OSs and NOSs, via the interaction between biogenic precursors and  
35 anthropogenic pollutants ( $\text{NO}_x$ ,  $\text{SO}_2$  and  $\text{SO}_4^{2-}$ ). The results imply that future reduction in anthropogenic emissions can help  
36 to reduce the biogenic SOA burden in Beijing or other areas impacted by both biogenic emissions and anthropogenic  
37 pollutants.

## 38 **1 Introduction**

39 Secondary organic aerosols (SOA), formed by atmospheric oxidation of volatile organic compounds (VOCs), accounts  
40 for a large fraction of organic aerosols (OA) on the global scale (Jimenez et al., 2009; Guo et al., 2014). However, current  
41 models usually underestimate (Kroll and Seinfeld, 2008; Hallquist et al., 2009) or predict the SOA concentration with large  
42 uncertainties (Jimenez et al., 2009; Kiehl, 2007; Shrivastava et al., 2017) in the ambient atmosphere. Thus, it is important to  
43 elucidate potential missing groups of compounds or formation mechanisms. Organosulfates (OSs), commonly formed via the  
44 interaction between VOC precursors and acidic sulfate seed particles, could be a potential source of “missing SOA” in  
45 current atmospheric models (Surratt et al., 2010). OSs have been observed in various ambient atmospheres, including urban,  
46 rural, suburban, forest as well as remote environments (Lin et al., 2012; Meade et al., 2016; Stone et al., 2012; Riva et al.,  
47 2015; Brüggemann et al., 2017), which could represent 2-30% of OA (Hawkins et al., 2010; Stone et al., 2012; Frossard et  
48 al., 2011; Tolocka and Turpin, 2012; Surratt et al., 2008; Liao et al., 2015).

49 Many prior chamber experiments revealed the precursors and formation mechanisms of OSs (Surratt et al., 2007;

50 Surratt et al., 2010; Surratt et al., 2008; Liggio and Li, 2006; Chan et al., 2011; Shalamzari et al., 2014; Shalamzari et al.,  
51 2016; Zhang et al., 2012), however, the atmospheric relevance of these remain unclear. Various biogenic VOCs (BVOCs)  
52 precursors have been reported, including isoprene (Hatch et al., 2011; Surratt et al., 2010), monoterpenes (Surratt et al.,  
53 2008), sesquiterpenes (Chan et al., 2011), pinonaldehyde (Liggio and Li, 2006), unsaturated aldehydes (Shalamzari et al.,  
54 2014; Shalamzari et al., 2016) and 2-methyl-3-buten-2-ol (Zhang et al., 2012). OSs originating from isoprene are some of the  
55 most studied compounds and could be among the most abundant OA in some areas (Liao et al., 2015; Chan et al., 2010;  
56 Surratt et al., 2010; Lin et al., 2013a; Worton et al., 2013). Isoprene OSs usually form through ring-opening epoxide  
57 chemistry catalyzed by acidic sulfate aerosols (Worton et al., 2013; Froyd et al., 2010; Paulot et al., 2009). OSs were also  
58 proposed to form by reactive uptake of VOCs or their oxidation products that involves the sulfate radicals (Nozière et al.,  
59 2010; Schindelka et al., 2013). The sulfate esterification of alcohols could also be a pathway leading to OSs formation, while  
60 Minerath et al (2018) predicted that this mechanism was kinetically insignificant under ambient tropospheric conditions.  
61 However, this prediction was based on laboratory bulk solution-phase experiments and the applicability to the liquid-phase  
62 on particles suspended in the air is unconfirmed. Nitrooxy organosulfates (NOSs) were observed to form via the nighttime  
63 NO<sub>3</sub>-initiated oxidation of VOC precursors (e.g. monoterpene), followed by alcohol sulfate esterification (Iinuma et al., 2007;  
64 Surratt et al., 2008). Organic nitrate (R-ONO<sub>2</sub>) could also act as precursors to OSs through the nucleophilic substitution of  
65 nitrate by sulfate (Hu et al., 2011; Darer et al., 2011).

66 Both aerosol acidity and liquid water content (LWC) are key variables influencing the OS formation processes. OS  
67 formation could only happen in the presence of sulfate aerosols, enhanced by increased aerosol acidity, through  
68 acid-catalyzed reactive uptake and multiphase reactions of oxidation products (Riva et al., 2016c; Surratt et al., 2010; Lal et  
69 al., 2012; Riedel et al., 2015). Previous studies also demonstrated the importance of aqueous-phase or heterogeneous  
70 reactions for OS formation (Lal et al., 2012; McNeill et al., 2012; McNeill, 2015; Riedel et al., 2015). On one hand, the  
71 increased LWC would decrease the aerosol viscosity, which favors the exchange of organics or other gas molecules into the  
72 particles, mass diffusion of reactants and heterogeneous chemical reactions within the particles (Vaden et al., 2011; Booth et  
73 al., 2014; Renbaum-Wolff et al., 2013; Shrestha et al., 2015; Zhang et al., 2015), and thereby enhance the OS formation. On  
74 the other hand, more LWC would lead to increased pH due to dilution. For example, Riva et al. (2016) and Duporte et al.

75 (2016) found that the OS formation decreased with higher RH, which was attributed to the increased pH as a result of higher  
76 LWC (Duporte et al., 2016; Riva et al., 2016c).

77 To get a comprehensive understanding of the characteristics and formation of OSs in the ambient atmosphere, it is  
78 desirable to simultaneously identify and quantify particulate OSs on the molecular level. Soft ionization techniques coupled  
79 with ultrahigh-resolution mass spectrometer (UHRMS) have been widely applied to identify various and numerous organics,  
80 including OS species, in ambient aerosols or chamber studies (Lin et al., 2012; Blair et al., 2017; Tao et al., 2014; Wang et al.,  
81 2016). UHRMS is a powerful analytical tool in gaining an overall characterization of OSs, however, the quantification  
82 capability is limited without pre-separation. High performance liquid chromatography coupled to mass spectrometer  
83 (HPLC-MS) is suitable for the separation and quantification of different OS compounds. However, one noted limitation is a  
84 lack of commercially available authentic standards. As a result, surrogate standards are often used for quantification (He et  
85 al., 2014; Riva et al., 2015; Zhang et al., 2012), which adds uncertainty to the concentrations (Wang et al., 2017d). Recently,  
86 a few research groups quantified some OS species using synthetic authentic standards (e.g. hydroxyacetone sulfate, glycolic  
87 acid sulfate, lactic acid sulfate, methyltetrol sulfate, aromatic OSs,  $\alpha/\beta$ -pinene OS, Limonene OS and Limonaketone OS)  
88 (Hettiyadura et al., 2017; Hettiyadura et al., 2015; Olson et al., 2011; Wang et al., 2017d; Ma et al., 2014; Budisulistiorini et  
89 al., 2015; Staudt et al., 2014), which was very important for understanding the variation and formation of OSs in ambient  
90 aerosols.

91 Missing knowledge of formation mechanisms, the complexities of ambient aerosol composition and oxidation condition,  
92 and the lack of commercially available standards all hinder us from understanding the formation and fate of OSs in ambient  
93 atmosphere. Few field studies has been conducted in urban areas dominated by anthropogenic pollutants (e.g.  $\text{NO}_x$ ,  $\text{SO}_4^{2-}$ ).  
94 Observations are lacking to illustrate how severe anthropogenic pollutants could influence the OS formation under different  
95 physical environmental conditions. This work reports a comprehensive characterization of particulate OSs in summertime  
96 Beijing, a location under the influence of both biogenic and severe anthropogenic sources. This study provides direct  
97 observational evidence for gaining insights into OS formation. Orbitrap MS coupled with soft ionization source was used to  
98 identify the overall molecular composition of S-containing organics. HPLC-MS was then applied to quantify some OSs and  
99 NOS species in ambient aerosols using newly synthesized authentic standards and surrogate standards. Previously proposed

100 formation pathways of OS or NOS (e.g. acid-catalyzed aqueous-phase chemistry, nighttime NO<sub>3</sub> chemistry) were considered,  
101 and the influence of different [environmental conditions](#) or factors on the formation were comprehensively elaborated. It has  
102 been suggested that both aqueous-phase chemistry and nighttime NO<sub>3</sub> chemistry play important roles in the heavy haze of  
103 Beijing (Wu et al., 2018; Wang et al., 2017b; Wang et al., 2017a). Using OSs and NOSs as examples, this work illustrates  
104 SOA formation via acid-catalyzed aqueous-phase chemistry, nighttime NO<sub>3</sub> chemistry under the interaction between  
105 abundant anthropogenic pollutants and biogenic emissions.

## 106 **2 Methods**

### 107 **2.1 Sample collection**

108 This study was a part of the bilateral Sweden-China framework research program on ‘Photochemical smog in China:  
109 formation, transformation, impact and abatement strategies’, focusing on the SOA formation under the influence of  
110 anthropogenic pollutants (Hallquist et al., 2016). An intensive field campaign was conducted at Changping (40.14° N,  
111 116.11° E), a regional site 38 km northeast of the Beijing urban area, China. The campaign was conducted from May 15 to  
112 June 23, 2016, when the site was influenced by high biogenic emissions from vegetation in the nearby mountains and  
113 anthropogenic pollutants from the nearby villages and Beijing urban areas (Tang et al., 2017). During May 17- June 5, the  
114 average concentrations of isoprene, monoterpenes, benzene, toluene and NO<sub>x</sub> were 297, 83, 441, 619 pptv and 22.7 ppb,  
115 respectively.

116 Ambient aerosols were collected from May 16 to June 5. PM<sub>2.5</sub> (particles with aerodynamic diameter less than 2.5 μm)  
117 samples were collected on prebaked quartz fiber filters (Whatman Inc.) and Teflon filters (Whatman Inc.) using a  
118 high-volume sampler (TH-1000C, Tianhong, China) and a 4-channel sampler (TH-16A, Tianhong, China), [respectively](#). The  
119 sampling flow rates were 1.05 m<sup>3</sup>/min and 16.7 L/min, respectively. The daytime samples were collected from 8:30 to 17:30  
120 and nighttime ones from 18:00 to 8:00 the next morning. Field blank samples were collected by placing filters in the  
121 samplers with the pump off for 30 min. The period May 20 - June 3 will be discussed in this study.

## 122 2.2 Orbitrap MS analysis

123 An Exactive Plus-Orbitrap MS (Thermo Scientific Inc., Bremen, Germany) equipped with a heated electrospray  
124 ionization (ESI) source was used to identify the overall molecular composition of OSs. Details of the extraction and data  
125 analysis have been described in Wang et al. (2017c). Briefly, a portion of filter was extracted with ultrapure water in an  
126 ultrasonic bath for 40 min and the extracts were filtered with 0.45  $\mu\text{m}$  pore size PTFE syringe filter (Gelman Sciences). The  
127 filter portion size was adjusted to yield  $\sim 200$   $\mu\text{g}$  OC in each extract, in order to decrease the variation of ion suppression  
128 arising from varying coexisting organic components. The influence of ion suppress was illustrated in the Appendix S1. The  
129 extract sample was then loaded onto a solid phase extraction (SPE) cartridge (DSC-18, Sigma-Aldrich, USA) to remove  
130 inorganic ions and low molecular weight (MW) organic acids (Lin et al., 2010), followed by elution with methanol. The  
131 methanol eluate was dried under a gentle stream of  $\text{N}_2$  and re-dissolved in acetonitrile/water (1:1) solvent for Orbitrap MS  
132 analysis. Some selected OS species of low MW (e.g., isoprene-derived OSs such as  $\text{C}_4\text{H}_7\text{O}_7\text{S}^-$ ,  $\text{C}_5\text{H}_7\text{O}_7\text{S}^-$ , and  $\text{C}_5\text{H}_{11}\text{O}_7\text{S}^-$ )  
133 would be removed by the SPE clean-up procedure and thus not detected by the direct infusion Orbitrap MS analysis (see  
134 section 3.1). We note that these OS species were detected by HPLC-MS in the sample extracts to which no SPE pretreatment  
135 procedure was applied (see section 2.3). This phenomenon was also reported in previous studies (Gao et al., 2006; Surratt et  
136 al., 2007).

137 The Orbitrap MS was operated in negative mode (ESI<sup>-</sup>). The mass calibration was conducted using a standard mixture  
138 of N-butylamine, caffeine, MAFA, sodium dodecyl sulfate, sodium taurocholate and Ultramark 1621, with the scan range set  
139 to be 90-900  $m/z$ . The Orbitrap MS had a mass resolving power of 140,000 at  $m/z = 200$ . Each sample was analyzed for three  
140 times with at least 100 full-scan spectra acquired in each analysis. The recorded mass spectra were processed and exported  
141 using the Xcalibur software (V2.2, Thermo Scientific). Peaks with a signal-to-noise ratio  $\geq 10$  were exported. All the  
142 mathematically possible formulas for each ion were calculated with a mass tolerance of 2 ppm. Each exported molecular  
143 formula was allowed containing certain elements and limited by several conservative rules (Wang et al., 2017c). Elements  
144  $^{12}\text{C}$ ,  $^1\text{H}$ ,  $^{16}\text{O}$ ,  $^{14}\text{N}$ ,  $^{32}\text{S}$  and  $^{13}\text{C}$  were allowed in the molecular formula calculations. The H/C, O/C, N/C and S/C ratios were  
145 limited to 0.3- 3.0, 0- 3.0, 0- 0.5 and 0- 2.0. The assigned formulas were also restrained by the double bond equivalent values

146 and the nitrogen rule for even electron ions. More details about the molecular formula assignment have been introduced in  
147 Wang et al. (2017c). The background spectra were obtained by analyzing the corresponding field blank sample following the  
148 same procedure. Peaks were eliminated from the list if their intensities were lower than ten times of those in the blank  
149 sample.

### 150 **2.3 Quantification of OSs and NOSs using HPLC-MS**

151 An aliquot of 25 cm<sup>2</sup> was removed from each filter sample and extracted in ultrasonic bath three times using 3, 2 and 1  
152 mL methanol consecutively, each time for 30 min. The extracts were then filtered through a 0.25 µm polytetrafluoroethylene  
153 (PTFE) syringe filter (Pall Life Sciences), combined, evaporated to dryness under a gentle stream of high-purity nitrogen and  
154 re-dissolved in 50 µL methanol/water (1:1) containing 1 ppm D<sub>17</sub>-octyl sulfate as internal standard. The solution was  
155 centrifuged and the supernatant was used for analysis, using Agilent 1260 LC system (Palo Alto, CA) coupled to QTRAP  
156 4500 (AB Sciex, Toronto, Ontario, Canada) mass spectrometer. The LC/MS was equipped with an ESI source operated in  
157 negative mode. The optimized MS conditions and details of the method have been described in our previous study (Wang et  
158 al., 2017d). Chromatographic separation was performed on an Acquity UPLC HSS T3 column (2.1 mm×100 mm, 1.8 µm  
159 particle size; Waters, USA) with a guard column (HSS T3, 1.8 µm). The mobile eluents were (A) water containing 0.1%  
160 acetic acid (v/v) and (B) methanol (v/v) containing 0.1% acetic acid at a flow rate of 0.19 mL/min. The gradient elution was  
161 set as follows: the composition started with 1% B for 2.7 min; increased to 54% B within 12.5 min and held for 1.0 min; then  
162 increased to 90% B within 7.5 min and held for 0.2 min; and finally decreased to 1% B within 1.8 min and held for 17.3 min  
163 until the column was equilibrated. The column temperature was kept at 45 °C and the injection volume was 5.0 µL.

164 The quantified OS and NOS species are listed in Table 1. The monoterpene NOSs (C<sub>10</sub>H<sub>16</sub>NO<sub>7</sub>S<sup>-</sup> and C<sub>9</sub>H<sub>14</sub>NO<sub>8</sub>S<sup>-</sup>) were  
165 quantified using the [M-H]<sup>-</sup> ions in the extracted ion chromatogram (EIC) and other species were quantified in  
166 multiple-reaction monitoring (MRM) mode. OSs and NOSs were quantified using authentic standards or surrogates with  
167 similar molecular structures (Table 1). Lactic acid sulfate (LAS) and glycolic acid sulfate (GAS) were prepared according to  
168 Olson et al. (2011). The purity of LAS and GAS are 8% and 15%, determined by <sup>1</sup>H NMR analysis using dichloroacetic acid  
169 as an internal standard, and the recovery are 89.5% and 94.9%, respectively. Four monoterpene derived OS standards were

170 synthesized and the details are given in Wang et al. (2017). The purity of the four monoterpene OS standards are higher than  
171 99% and the recovery are 80.5%-93.5% (Table S1). OSs with similar carbon chain structures usually have similar MS  
172 responses (Wang et al., 2017d). Lactic acid sulfate was employed as a surrogate standard to quantify isoprene OSs due to  
173 their similar structures and retention times (Table 1).  $\alpha$ -pinene OS and limonaketone OS were respectively used to quantify  
174 monoterpene NOSs  $C_{10}H_{16}NO_7S^-$  and  $C_9H_{14}NO_8S^-$  due to the similar carbon structures (Table 1). For the molecule with  
175 isomers, quantification was performed by summing up the peak areas of the isomers, treated as one species (e.g.,  
176 monoterpene NOSs with  $[M-H]^-$  at  $m/z$  294 were treated as one NOS species).

## 177 **2.4 Other online and offline measurements**

178 A high resolution time-of-flight aerosol mass spectrometer (AMS) was employed to measure the chemical composition  
179 of  $PM_{1.0}$ . The operation procedures and data analysis have been described in Zheng et al. (2017). VOCs were measured by a  
180 proton-transfer-reaction mass spectrometer (PTR-MS). Meteorological parameters, including relative humidity (RH),  
181 temperature, wind direction and wind speed (WS) were continuously monitored by a weather station (Met one Instrument  
182 Inc.) during the campaign. Organic carbon (OC) was analyzed using thermal/optical carbon analyzer (Sunset Laboratory).  
183 The organic matter (OM) concentration was calculated by multiplying OC by 1.6 (Turpin and Lim, 2001). Water soluble  
184 inorganic ions and low MW organic acids (e.g. oxalic acid) were quantified by an ion chromatograph (IC, DIONEX,  
185 ICS2500/ICS2000) following procedures described in Guo et al. (2010). After performing quality assurance/quality control  
186 for IC measurements, the data (ions, pH, LWC) derived from IC measurements in the daytime samples of May 26 and 29  
187 were excluded in the following analysis. Gaseous  $NH_3$  was measured using a  $NH_3$  analyzer (G2103, Picarro, California,  
188 USA) (Huo et al., 2015). Aqueous phase  $[H^+]$  and LWC were then calculated with the ISORROPIA-II thermodynamic  
189 model. ISORROPIA-II was operated in forward mode, assuming the particles are “metastable” (Hennigan et al., 2015;  
190 Weber et al., 2016; Guo et al., 2015). The input parameters included: ambient RH, temperature, particle phase inorganic  
191 species ( $SO_4^{2-}$ ,  $NO_3^-$ ,  $Cl^-$ ,  $NH_4^+$ ,  $K^+$ ,  $Na^+$ ,  $Ca^{2+}$ ,  $Mg^{2+}$ ), and gaseous  $NH_3$ . The thermodynamic calculations were validated by  
192 the good agreement between measured and predicted gaseous  $NH_3$  (slope=0.99,  $R^2=0.97$ ) (see Appendix S2 for details). The  
193 contribution of organics to LWC was not considered in this study. Our previous study in Beijing has suggested that LWC

194 associated with organic species was insignificant (<6%), compared to that of secondary inorganic aerosols (Wu et al., 2018)  
195 (see Fig. S3 for the comparison between LWC with or without water associated with organic compounds). Previous study  
196 also suggested that the predicted aerosol acidity or pH without consideration of organic water could also be sufficient for  
197 discussing aqueous SOA chemistry in this study, due to the minor effect on aerosol pH (0.15- 0.23) (Guo et al., 2015).

## 198 **3 Results and discussion**

### 199 **3.1 Overall molecular characterization of S-containing organics**

200 On average, 62% of the observed peaks in ESI negative mode are assigned with unambiguous molecular formulas. All  
201 the assigned formulas were classified into four major categories based on their elemental compositions, including CHO,  
202 CHON, CHOS and CHONS. As an example, CHONS refers to compounds that contain C, H, O, N and S elements in the  
203 formula. Other compound categories are defined analogously. The percent of different compound categories in terms of  
204 number and intensity are shown in Fig. S4 and Fig. 1, in which ‘others’ (e.g. CH, CHN, CHS, CHNS) refer to the  
205 compounds excluded from the above major compound categories. During pollution episodes, the number and intensity  
206 percent of S-containing compounds (CHOS and CHONS) increased obviously (Fig. 1, S4). The OC content in each sample  
207 for Orbitrap MS analysis was kept roughly constant to minimize variation arising from matrix ion suppression. Taking the  
208 nighttime sample of May 24 (0524N) as an example of clean days and the nighttime sample of May 30 (0530N) as an  
209 example of polluted days, the mass spectra of different compound categories in each sample are shown and compared in Fig.  
210 1 (a) and (b). The increase in S-containing organics indicated their important contribution to SOA when the pollution  
211 accumulated. What’s more, the S-containing compounds contributed more to the higher MW formulas than CHO ( $O_1$ - $O_{10}$ ) or  
212 CHON ( $O_1$ - $O_{11}$ ) compounds (Fig. 1), due to the existence of more O (CHOS:  $O_1$ - $O_{12}$ , CHONS:  $O_1$ - $O_{14}$ ) atoms and  
213 heteroatoms (S, N) in the molecules. The increasing trend of S-containing organics (Fig S4), with larger MW than those of  
214 CHO or CHON, may play important roles in the increase of SOA mass concentrations during pollution episodes.

215 The CHOS formulas with  $O/S \geq 4$  allow the possible assignment of a sulfate group in the molecules (i.e., OSs) (Lin et  
216 al., 2012). Among all the identified CHOS formulas, 60%-99% (93% on average) and 66-100% (96% on average) of them

217 could be assigned as OSs in terms of number and intensity percent. Analogously, the CHONS formulas with  $O/(S+N) \geq 7$   
218 could likely be NOSs formulas, which account for 22-78% (53% on average) by number and 18-94% (61% on average) by  
219 intensity of all the identified CHONS formulas. As OSs and NOSs were assigned based on the molecular formulas alone, we  
220 could not completely exclude the possibility of CHOS being hydroxysulfonates and CHONS being nitro-OSs due to the lack  
221 of MS/MS analysis. According to previous study, the presences of organosulfonate or nitro-OSs were usually limited  
222 compared to those of OSs or nitrooxy-OSs (Lin et al., 2012), thus they were not taken into consideration in this study. A total  
223 of 351 OSs and 181 NOSs formulas were identified among all the samples during the campaign. The temporal variation of  
224 the total number and intensity of OSs and NOSs are shown in Fig. S4. During pollution episodes (nighttime of May 27 - the  
225 nighttime of May 28, nighttime of May 29 - the nighttime of May 30), the total number and intensity of OSs formulas  
226 increased (Fig. S4). The total number of NOSs also showed similar increase trend during pollution episodes, while the total  
227 intensity of NOSs showed nighttime enhancement during the whole observation period (Fig. S4). Previous studies suggested  
228 that some NOS species could form via  $\text{NO}_3$ -initiated oxidation under high- $\text{NO}_x$  conditions at night (Surratt et al., 2008;  
229 Iinuma et al., 2007; Gomez-Gonzalez et al., 2008), which will be further discussed in the following sections.

230 Some of the more abundant OSs and NOS peaks identified in the samples on the clean day (05/24N) or during pollution  
231 episodes (05/30D, 05/30N) are listed in Table S2. For example, deprotonated molecules  $\text{C}_9\text{H}_{15}\text{SO}_7^-$ ,  $\text{C}_{10}\text{H}_{17}\text{SO}_7^-$  and  
232  $\text{C}_9\text{H}_{17}\text{SO}_6^-$  were observed among the highest OS peaks in samples during pollution episodes (Table S2). These compounds  
233 could be derived from the oxidation of alkanes or diesel fuel based on previous chamber studies (Riva et al., 2016c; Blair et  
234 al., 2017). Many OSs previously designated as biogenic origins were also found in the anthropogenic sources (Blair et al.,  
235 2017), which may raise uncertainty when assigning OS sources in field observation studies. OS compounds derived from  
236 anthropogenic VOC precursors were widely observed in ambient aerosols (Table S2), while they were not quantified due to  
237 the lack of standards in this paper. They will be further investigated in our future studies. Other OS molecules (e.g.  
238  $\text{C}_9\text{H}_{15}\text{SO}_6^-$ ,  $\text{C}_{10}\text{H}_{17}\text{SO}_5^-$ ) could be formed via the oxidation of monoterpenes (Surratt et al., 2008). For NOSs, ions  
239  $\text{C}_{10}\text{H}_{16}\text{NO}_7\text{S}^-$ ,  $\text{C}_{10}\text{H}_{16}\text{NO}_9\text{S}^-$  and  $\text{C}_{10}\text{H}_{16}\text{NO}_{10}\text{S}^-$  were among the highest peaks (Table S2). They could form via the nighttime  
240  $\text{NO}_3$ -initiated oxidation of monoterpenes (Surratt et al., 2008). These are just some examples with higher relative intensity  
241 (RI). The RI may not accurately represent their relative concentration levels in each sample, as the MS responses of different

242 OSs are also influenced by different carbon chain structures (Wang et al., 2017d). The OS species of low MW and short  
243 carbon chain structures (with fewer than 6 carbon atoms in the molecule) are little retained on the SPE cartridges due to their  
244 highly water-soluble and more hydrophilic properties (Gomez-Gonzalez et al., 2008; Lin et al., 2012; Lin et al., 2010). As  
245 such, they were largely absent among the OS formulas detected by Orbitrap MS in this work. Hydroxyacetone sulfate  
246 ( $C_3H_5O_5S^-$ ) was detected by Orbitrap MS only in several samples with relatively higher concentrations. Hydroxycarboxylic  
247 acid sulfate ( $C_2H_3O_6S^-$ ,  $C_3H_5O_6S^-$ ) or isoprene OSs ( $C_4H_7O_7S^-$ ,  $C_5H_7O_7S^-$ ,  $C_5H_{11}O_7S^-$ ) are also sufficiently hydrophilic that  
248 little of them would be in the SPE eluate fraction, which was subjected for Orbitrap MS analysis. This explains why these  
249 highly water-soluble OS species with lower MW are absent in Fig. 1. Though these OS species were not detected by Orbitrap  
250 MS, some of them were quantified with high concentrations in the ambient aerosols in the LC/MS analysis (Table 1), as the  
251 sample aliquots for the LC/MS analysis did not involve SPE treatment.

### 252 3.2 Abundance of identified OSs and NOSs in ambient aerosols

253 To further investigate the abundance and formation pathways of OSs and NOSs in ambient aerosols, some species were  
254 then quantified by HPLC-MS using authentic standards when available or surrogate standards. The quantified species could  
255 usually be formed via the interaction between biogenic precursors (e.g. isoprene, monoterpene) and anthropogenic pollutants  
256 (e.g.  $SO_4^{2-}$ ,  $NO_x$ ), which have been reported in previous chamber studies (Surratt et al., 2007; Surratt et al., 2008; Surratt et  
257 al., 2010). A total of ten OSs and three NOS species were quantified in this study and their concentrations are listed in Table  
258 1. The molecules with the same molecular formula were treated as one species (e.g., monoterpene NOSs with  $[M-H]^-$  at  $m/z$   
259 294 were treated as one NOS species). The average concentrations of all the quantified OSs were  $41.4 \text{ ng/m}^3$  during the  
260 campaign. The total OSs accounted for 0.31% of OM, with a maximum contribution of 0.65% on the night of May 30. The  
261 total concentrations of quantified NOSs were  $13.8 \text{ ng/m}^3$ , corresponding to 0.11% of OM, with a maximum contribution of  
262 0.35% on the night of May 23.

263 The concentrations of each OS or NOS species across this and prior studies were summarized in Table S3. The relative  
264 contribution of each species to the total OSs or NOSs is shown in Fig. 2. GAS was the most abundant species among all the  
265 quantified species. The concentrations of GAS were  $3.9\text{-}58.2 \text{ ng/m}^3$ , with an average of  $19.5 \text{ ng/m}^3$ . The concentrations were

266 higher than those observed in Mexico (4.1- 7.0 ng/m<sup>3</sup>), California (3.3- 5.4 ng/m<sup>3</sup>) or Pakistan (11.3 ng/m<sup>3</sup>) (Olson et al.,  
267 2011) (Table S3). The GAS concentration level at Beijing was comparable to those reported in summertime Alabama, US  
268 (8-26.2 ng/m<sup>3</sup>) (Table S3), a location characterized by high biogenic emissions and affected by anthropogenic pollutants  
269 (Hettiyadura et al., 2015; Hettiyadura et al., 2017; Rattanavaraha et al., 2016). The concentrations of LAS were 0.7-12.0  
270 ng/m<sup>3</sup>, with an average of 4.4 ng/m<sup>3</sup>. The LAS concentrations were also higher than those observed in Mexico (1.2-1.8  
271 ng/m<sup>3</sup>), California (0.6-0.8 ng/m<sup>3</sup>) or Pakistan (3.8 ng/m<sup>3</sup>), while lower than those observed in Alabama, US (16.5 ng/m<sup>3</sup>)  
272 (Olson et al., 2011; Hettiyadura et al., 2015; Hettiyadura et al., 2017) (Table S3). Carboxylic acids mainly form via  
273 aqueous-phase oxidation in cloud or particle water, including both biogenic and anthropogenic sources (Charbouillot et al.,  
274 2012; Chebbi and Carlier, 1996). The relatively higher level of hydroxycarboxylic acid sulfate could be attributed to the  
275 favorable interaction between sulfate aerosols and carboxylic acids or other precursors in summertime Beijing, while the  
276 precursors and mechanisms remain unclear. Oxalic acid is usually the most abundant dicarboxylic acid in the atmosphere  
277 (Guo et al., 2010; Narukawa et al., 2003). The average concentration of oxalic acid in fine particles was 0.22 μg/m<sup>3</sup>, which  
278 was at a relatively high concentration level when comparing with those reported in previous studies (0.02-0.32 μg/m<sup>3</sup>)  
279 (Agarwal et al., 2010; Bikkina et al., 2017; Boreddy et al., 2017; Deshmukh et al., 2017; Kawamura et al., 2010; Narukawa  
280 et al., 2003). Strong inter-correlations were found among GAS, LAS and hydroxyacetone sulfate (HAS) (Table S4),  
281 indicating their potentially similar precursors or formation pathways. They also showed strong correlations with isoprene  
282 oxidation products (MVK+MACR) and isoprene OSs (Table S4), suggesting isoprene oxidized products as potential  
283 precursors of GAS, LAS and HAS. It is suggested that both hydroxyacetone and carboxylic acids could be produced from  
284 the oxidation of isoprene (Fu et al., 2008; Carlton et al., 2009). GAS, LAS and HAS have been reported to form via isoprene  
285 oxidation in the presence of acidic sulfate (Riva et al., 2016b; Surratt et al., 2008). GAS was also observed to form via  
286 sulfate induced oxidation of methyl vinyl ketone (MVK), oxidation product of isoprene (Schindelka et al., 2013).

287 The concentration of quantified isoprene OSs (C<sub>4</sub>H<sub>7</sub>O<sub>7</sub>S<sup>-</sup>, C<sub>5</sub>H<sub>7</sub>O<sub>7</sub>S<sup>-</sup> and C<sub>5</sub>H<sub>11</sub>O<sub>7</sub>S<sup>-</sup>) was 14.8 ng/m<sup>3</sup>, contributing to 36 %  
288 of the total quantified OSs in this study. The isoprene OSs were lower than those observed in southeastern US, with  
289 substantial isoprene emissions and impacted by anthropogenic pollutants, in which authentic standards were employed to  
290 quantify the isoprene OSs (Rattanavaraha et al., 2016). We used lactic acid sulfate as a surrogate standard to quantify

291 isoprene OSs on the basis of their similar structures and retention times (Table 1). The isoprene concentration in southeastern  
292 US (1.9 ppb) (Xu et al., 2015) was much higher than that observed during our campaign (297 pptv). Besides the lower VOC  
293 precursors and measurement uncertainty, the lower isoprene OSs in this study could be attributed to different atmospheric  
294 conditions in Beijing from those in southeastern US. The IEPOX formation under low-NO<sub>x</sub> conditions (HO<sub>2</sub> channel),  
295 usually with higher yields than the oxidation products under high-NO<sub>x</sub> conditions (NO/NO<sub>2</sub>) (Worton et al., 2013), could be  
296 suppressed under the high-NO<sub>x</sub> conditions (see section 3.4 for the high-NO<sub>x</sub> conditions) in Beijing (Zhang et al., 2017; Hu et  
297 al., 2015). The RH in Beijing was lower than that in southeast US (Xu et al., 2015), which possibly led to an increase of  
298 aerosol viscosity and a decrease of diffusivity within the particles, resulting in lower OS formation (Shiraiwa et al., 2011).  
299 Moreover, the OM-coated particle structures observed in Beijing could reduce the reactive uptake of isoprene oxidation  
300 products (Li et al., 2016; Zhang et al., 2018; Riva et al., 2016a), which may be another possible reason for lower isoprene  
301 OSs in this study. The concentrations were comparable to those observed in suburban area of mid-Atlantic or Belgium and  
302 higher than those observed at the background site of Pearl River Delta (PRD) region, China (Meade et al., 2016;  
303 Gómez-González et al., 2012; He et al., 2014), in which glycolic sulfate ester, ethanesulfonic acid or camphor sulfonic acid  
304 were employed as surrogate standards. The isoprene OSs formed via HO<sub>2</sub> channel (C<sub>5</sub>H<sub>11</sub>O<sub>7</sub>S<sup>-</sup>) were observed to be higher  
305 than that formed via NO/NO<sub>2</sub> channel (C<sub>4</sub>H<sub>7</sub>O<sub>7</sub>S<sup>-</sup>) (Table 1) (Worton et al., 2013). Isoprene had higher mixing ratio during  
306 the daytime (Fig. S5 (b)), when OH radicals dominated the atmospheric oxidation capacity. Furthermore, the yield of  
307 isoprene oxidation via HO<sub>2</sub> channel is proposed to be higher than that via NO/NO<sub>2</sub> channel (Worton et al., 2013). The  
308 concentration of C<sub>5</sub>H<sub>7</sub>O<sub>7</sub>S<sup>-</sup> was comparable to that of C<sub>5</sub>H<sub>11</sub>O<sub>7</sub>S<sup>-</sup> (Table 1). C<sub>5</sub>H<sub>7</sub>O<sub>7</sub>S<sup>-</sup> was suggested to be formed via  
309 isoprene oxidation and related to C<sub>5</sub>H<sub>11</sub>O<sub>7</sub>S<sup>-</sup> (Surratt et al., 2008), while the formation mechanism remains unclear. The  
310 concentration of isoprene NOSs (C<sub>5</sub>H<sub>10</sub>NO<sub>9</sub>S<sup>-</sup>) was lower than that of individual isoprene OSs. Strong inter-correlations were  
311 observed between isoprene OSs and NOSs (Table S4), suggesting their similar formation pathways via acid-catalyzed  
312 epoxide chemistry (Worton et al., 2013).

313 The average concentration of monoterpene OSs ( $\alpha$ -pinene OSs,  $\beta$ -pinene OSs, limonene OSs and limonaketone OSs)  
314 was 0.6 ng/m<sup>3</sup>, lower than those observed in mid-Atlantic (Meade et al., 2016) or the Pearl River Delta in southern China  
315 where more abundant emissions of BVOC precursors are expected (Wang et al., 2017d; He et al., 2014) (Table S3). The

316 contribution of monoterpene OSs was much lower than that of isoprene OSs or other OSs (Fig. 2, Table 1), as the mixing  
317 ratio of monoterpene (83 pptv) was lower than that of isoprene (297 pptv) during the campaign. Furthermore, the reactivity  
318 of monoterpenes with OH radical is lower than that of isoprene (Carlton et al., 2009; Paulot et al., 2009; Atkinson et al.,  
319 2006). Different from isoprene OSs, the four monoterpene OS species didn't show strong correlations with each other (Table  
320 S4), which may suggest their different oxidation mechanisms. While the contribution of monoterpene OSs was low, the  
321 monoterpene NOSs ( $C_{10}H_{16}NO_7S^-$ ) were the second most abundant signals among the observed species (Table 1, Table S2),  
322 especially in the nighttime samples. The concentration of monoterpene NOSs ( $C_{10}H_{16}NO_7S^-$ ) was much higher than those  
323 observed in mid-Atlantic or Belgium (Meade et al., 2016; Gómez-González et al., 2012), while lower than that observed in  
324 Pearl River Delta, South China (He et al., 2014).  $C_{10}H_{16}NO_7S^-$  was also identified to be among the highest peaks in the mass  
325 spectra recorded by Orbitrap MS (Fig. 1 (b)), with a RI of 83% in the sample of 05/30N (Table S2). The monoterpene NOSs  
326 could be formed via nighttime  $NO_3$ -initiated oxidation under high- $NO_x$  conditions (Surratt et al., 2008; Iinuma et al., 2007;  
327 Gomez-Gonzalez et al., 2008). During the observation, both monoterpenes and  $NO_x$  showed higher mixing ratios at night  
328 (Fig. S5 (a), (d)), favorable for the  $NO_3$ -initiated formation of NOSs.

### 329 **3.3 OS formation via acid-catalyzed aqueous-phase chemistry**

330 The time series of the total OS concentrations quantified by HPLC-MS are shown in Fig. 3, along with the  
331 meteorological conditions,  $SO_2$ , aerosol LWC, acidity,  $PM_{2.5}$  and the major chemical components. Most OS species showed  
332 similar trends to the total OSs (Fig. S6), except for  $\alpha$ -pinene OSs and  $\beta$ -pinene OSs, observed at very low concentrations.  
333 During the campaign, particles were generally acidic with a pH range of 2.0- 3.7, favorable for OS formation (Fig. 3). The  
334 aerosol acidity is indicated by aqueous phase  $[H^+]$  in this study. The OS concentrations generally followed a similar trend to  
335 that of sulfate aerosols (Fig. 3). The total OS concentrations showed strong correlations with sulfate ( $r=0.67$ ) or aerosol  
336 acidity ( $r=0.67$ ), suggesting the driving role of acidic sulfate aerosols in the OS formation (Table S4).

337 During the observation period, three pollution episodes (episodes I, II, III) were identified based on the  $PM_{2.5}$   
338 concentrations, which are marked by gray shadow in Fig. 3. The back trajectories, average concentrations of VOC precursors  
339 and oxidants during each episode are also shown in Table S5. The most significant increase trend of OSs was observed

340 during pollution episode III (nighttime of May 29 - the nighttime of May 30). During this episode, the accumulation of  
341 secondary inorganic aerosols (SIAs), referring to sulfate, nitrate and ammonium in this study, was dominated by sulfate.  
342 SIAs, especially sulfate and nitrate salts, represent the most important components driving the particle hygroscopicity (Wu et  
343 al., 2018; Xue et al., 2014), thus the aerosol LWC increased with SIAs (Fig. 3). The increase of aerosol acidity was also  
344 observed during this episode (Fig. 3). OSs increased to the highest level ( $129.2 \text{ ng/m}^3$ ) during the campaign under the  
345 condition of high sulfate aerosols, high aerosol acidity and LWC (Fig. 3), suggesting the acid-catalyzed aqueous-phase  
346 formation of OSs in the presence of acidic sulfate aerosols. The higher aerosol LWC encountered during these periods would  
347 also favor the uptake of gas-phase reactants into particle phase, due to the decrease of viscosity and increase of diffusivity  
348 within the particles (Shiraiwa et al., 2011). Moreover, the oxidant levels, indicated by  $\text{O}_x$  ( $\text{NO}_2 + \text{O}_3$ ) in this study (Herndon et  
349 al., 2008), were much higher than the other two episodes, which favored the formation of VOC oxidation products (e.g.  
350 MVK+MACR) (Table S5). This is another reason for higher OSs concentration level during episode III. During pollution  
351 episode II (nighttime of May 27 - the nighttime of May 28), the OS concentration level was lower than that during episode  
352 III. It is noted that the increase of sulfate, aerosol LWC and acidity were also less than that during episode III, indicating less  
353 aqueous-phase formation of OSs. During this episode, the increase of SIAs was attributed to both sulfate and nitrate, the two  
354 with comparable contribution to the total SIAs. Different from episodes II and III, the SIAs accumulation was dominated by  
355 nitrate during episode I (May 21- 23). OS and sulfate aerosols stayed at medium concentration level, lower than those during  
356 the other two episodes. During the daytime of May 21, aerosol acidity increased due to the elevated relative contribution of  
357 sulfate than that of nitrate, thus the OS concentration also increased. During the daytime of May 23, higher aerosol LWC  
358 was observed due to the rapid increase of nitrate, however, the aerosol acidity was lower as a result of the less contribution  
359 from sulfate. Thus, the increase of OS concentration was not very obvious. The OS formation may be limited by the aerosol  
360 acidity, indicating the importance of acid-catalyzed chemistry. Stronger correlations between OSs and sulfate ( $r=0.67$ ) or  
361 aerosol acidity ( $r=0.67$ ) compared with that between OSs and LWC ( $r=0.55$ ) also suggest the importance of acid-catalyzed  
362 chemistry for OSs formation. The back trajectories during episode I were different from those during episode II or III (Table  
363 S5), which could be one reason for different conditions (e.g. SIA composition) during episode I. This episode ended with the  
364 rain elimination event on the afternoon of May 23. The OSs were at low concentrations from May 24 to the daytime of May

365 27, when sulfate, SO<sub>2</sub>, aerosol acidity and LWC were noticeably lower than the other periods, restraining the OS formation.

366 The three pollution episodes were characterized by different inorganic aerosol composition and aerosol properties (e.g.  
367 acidity, LWC), resulting in different levels of OS formation. The concentrations and relative contribution of sulfate, aerosol  
368 acidity and LWC are important factors influencing OS formation. The OS concentrations generally increased with the  
369 increasing of sulfate, aerosol acidity and LWC (Fig. 3), suggesting more active OS formation via acid-catalyzed  
370 aqueous-phase reactions in the presence of sulfate. These influencing factors were interrelated. Both sulfate and nitrate are  
371 important hygroscopic components (Chan and Chan, 2005; Wu et al., 2018; Xue et al., 2014), favoring the water uptake of  
372 aerosols and thus increasing LWC. The increasing of aerosol LWC with SIAs was observed (Fig. 3). A previous study also  
373 suggested that at a given RH, aerosol LWC was nearly linearly related to the sum of nitrate and sulfate mass concentrations  
374 (Guo et al., 2016). The variation of SIA composition and LWC would then influence the aerosol acidity (Liu et al., 2017;  
375 Guo et al., 2016). In this study, higher aerosol acidity was observed with elevated contribution of sulfate among SIAs (Fig.  
376 3). This is in accord with a previous study suggesting that particle pH was generally below 2 when aerosol anionic  
377 composition was dominated by sulfate ( $\text{NO}_3^-/2\text{SO}_4^{2-}$  mole ratio >1) (Guo et al., 2016).

378 To further elucidate the major factors influencing OS formation and their interrelations with SIA compositions, the  
379 distribution of OS concentrations as a function of SO<sub>4</sub><sup>2-</sup>/SIAs mass concentration ratios and other related factors are plotted  
380 in Fig. 4. The aerosol LWC generally increased with the increasing of the SIA mass concentrations, while the aerosol acidity  
381 was also influenced by the relative contribution of SO<sub>4</sub><sup>2-</sup> and NO<sub>3</sub><sup>-</sup> to SIAs. When the SIAs were dominated by SO<sub>4</sub><sup>2-</sup>  
382 (SO<sub>4</sub><sup>2-</sup>/SIAs > 0.5), the aerosol acidity increased obviously as a function of SO<sub>4</sub><sup>2-</sup>/SIAs mass concentration ratios and the pH  
383 values were generally below 2.8 (Fig. 4 (b, d)). The high aerosol acidity was favorable for OS formation and OS  
384 concentration also increased as a function of sulfate mass concentration and fraction (Fig. 4 (a)). The pollution episode III  
385 (Fig. 3) was the typical case for this condition. When the SIAs were dominated by nitrate (SO<sub>4</sub><sup>2-</sup>/SIAs < 0.5), high LWC may  
386 occur due to the high concentrations of hygroscopic SIAs, while the aerosol acidity was relatively lower due to the lower  
387 sulfate fraction than that of nitrate (Fig. 4). The increase trend of OSs as a function of sulfate or SO<sub>4</sub><sup>2-</sup>/SIAs mass  
388 concentration ratios was not as obvious as the sulfate-dominant condition (SO<sub>4</sub><sup>2-</sup>/SIAs > 0.5), as the OS formation may be  
389 limited by lower aerosol acidity. The daytime of May 23 during pollution episode I (Fig. 3) was the typical case for this

390 atmospheric condition. Overall, the OS formation would obviously be promoted via acid-catalyzed aqueous-phase reactions,  
391 when the SIAs accumulation was dominated by sulfate ( $\text{SO}_4^{2-}/\text{SIAs} > 0.5$ ).

### 392 **3.4 Monoterpene NOS formation via the nighttime $\text{NO}_3$ oxidation**

393 A recent study suggested that nearly all the BVOCs could be oxidized overnight, dominated by reactions via  $\text{NO}_3$   
394 oxidation, at a  $\text{NO}_x/\text{BVOCs}$  ratio higher than 1.4 (Edwards et al., 2017). When we roughly estimated the BVOCs  
395 concentration to be the sum of isoprene, MVK+MACR, and monoterpenes, the  $\text{NO}_x/\text{BVOCs}$  ratios were higher than 10 at  
396 night (Fig. S5). This indicated the dominant nighttime BVOCs loss via  $\text{NO}_3$ -initiated oxidation in summer of Beijing. The  
397 oxidation of BVOCs was found to be controlled by  $\text{NO}_3$  oxidation rather than  $\text{O}_3$  oxidation during the campaign, which  
398 contributed to a total of 90% of BVOCs reactivity at night (Wang et al., 2018). Nighttime enhancement of monoterpene  
399 NOSs was clearly observed under high- $\text{NO}_x$  conditions (Fig. 5). The nighttime concentrations of  $\text{C}_{10}\text{H}_{16}\text{NO}_7\text{S}^-$  and  
400  $\text{C}_9\text{H}_{14}\text{NO}_8\text{S}^-$  were respectively 1.3-31.4 (9.8 on average) and 0.9-19.7 (5.8 on average) times larger than daytime  
401 concentrations. Higher mixing ratios of monoterpenes were observed at night (Fig. S5), when the high  $\text{NO}_x$  concentrations  
402 (Fig. 5) favored the formation of monoterpene NOSs via  $\text{NO}_3$ -initiated oxidation of monoterpenes. The elevated nighttime  
403 concentrations of monoterpene NOSs was also observed in previous studies (Surratt et al., 2008; Iinuma et al., 2007;  
404 Gomez-Gonzalez et al., 2008). High correlation between  $\text{N}_2\text{O}_5$  and  $\text{NO}_2$  or  $\text{NO}_3$  radical production were observed (Wang et  
405 al., 2018), so the  $\text{NO}_2$  concentration was employed to investigate  $\text{NO}_3$  oxidation during the campaign in this study. Higher  
406 concentrations of monoterpene NOSs ( $\text{C}_{10}\text{H}_{16}\text{NO}_7\text{S}^-$ ) were found with elevated  $\text{NO}_2$  levels at night (Fig. 6), indicating the  
407 plausibility of more NOS formation via  $\text{NO}_3$ -initiated oxidation. When  $\text{NO}_2$  increased to higher than 20 ppb, the NOS  
408 concentration did not further increase obviously with  $\text{NO}_2$ , which suggested that  $\text{NO}_2$  was in excess and no longer the  
409 limiting factor in NOS formation. The highest nighttime concentration of  $\text{C}_{10}\text{H}_{16}\text{NO}_7\text{S}^-$  was recorded on May 27 during  
410 episode II (Fig. 5). Besides the high  $\text{NO}_2$  concentration (>20 ppb), the high monoterpene level was another primary reason  
411 for the elevated concentration of monoterpene NOSs (Table S5).

412 The lower concentrations of monoterpene NOSs during the daytime could be attributed to the lower monoterpene,  $\text{NO}_x$   
413 and  $\text{NO}_x/\text{BVOCs}$  ratios than those at night (Fig. S5). What's more, monoterpene NOSs, also as organic nitrate ( $\text{R-ONO}_2$ )

414 compounds, may go through decomposition via photolysis or OH oxidation during the daytime (He et al., 2011;  
415 Suarez-Bertoa et al., 2012). Organic nitrates have been estimated to have a short lifetime of several hours (Lee et al., 2016).  
416 Elevation in concentrations of monoterpene NOSs were also observed with the increasing of NO<sub>2</sub> during daytime, but the  
417 concentrations were much lower and the increase was less prominent than that during the nighttime (Fig. 6). The highest  
418 daytime concentration of C<sub>10</sub>H<sub>16</sub>NO<sub>7</sub>S<sup>-</sup> was recorded on May 23 (10.6 ng/m<sup>3</sup>), followed by the daytime of May 31 (8.0  
419 ng/m<sup>3</sup>). The NO<sub>2</sub> concentrations were in the range of 20-25 ppb and 10-15 ppb during the daytime of May 23 and 31,  
420 respectively. It is noted that the J(O<sup>1</sup>D) values during the daytime of May 23 and 31 were much lower than other daytime  
421 periods (Fig. 5), indicating the possibility of less decomposition of monoterpene NOSs. Previous studies also reported that  
422 the organic nitrate have much shorter lifetimes than the corresponding OSs, thus it is possible that organic nitrates derived  
423 from monoterpene would undergo nucleophilic attack by sulfate and form monoterpene OSs or NOSs (He et al., 2014; Darer  
424 et al., 2011; Hu et al., 2011). Monoterpene NOSs could also undergo hydrolysis and form monoterpene OSs (Darer et al.,  
425 2011; Hu et al., 2011). These may be other potential pathways for the loss of monoterpene NOSs and production of  
426 monoterpene OSs. These potential formation pathways of monoterpene OSs were different from the formation pathways via  
427 acid-catalyzed aqueous-phase reactions. This could be another explanation for the different temporal variations of some  
428 monoterpene OSs (Fig. S6) from other OSs.

### 429 **3.5 Formation pathways of isoprene OSs and NOSs**

430 Different from the day-night variation trend of monoterpene NOSs, isoprene NOSs (C<sub>5</sub>H<sub>11</sub>NO<sub>9</sub>S<sup>-</sup>) displayed similar  
431 temporal variation to isoprene OSs and the total OSs (Fig. 7). Formation of the isoprene NOSs are supposed to have similar  
432 limiting factors to those affecting isoprene OSs, rather than those limiting the nighttime NO<sub>3</sub>-initiated formation of  
433 monoterpene NOSs. The strong correlation between isoprene OSs and NOSs also indicated their similar formation pathways  
434 or limiting factors in the formation (Table S4). The oxidation of isoprene could form isoprene epoxydiols (IEPOX),  
435 hydroxymethyl-methyl-lactone (HMML) or methacrolein (MACR) and methacrylic acid epoxide (MAE) (Paulot et al., 2009;  
436 Lin et al., 2013b; Worton et al., 2013; Nguyen et al., 2015). Both isoprene OSs and NOSs showed strong correlations with  
437 isoprene oxidation products (MVK+MACR) (Table S4). The isoprene OSs could be formed through ring-opening epoxide

438 reactions of isoprene oxidation products, which was shown to be a kinetically feasible pathway (Minerath and Elrod, 2009;  
439 Worton et al., 2013). Isoprene OSs were also proposed to form by reactive uptake and oxidation of MVK or MACR  
440 (oxidation products of isoprene) initiated by the sulfate radicals (Nozière et al., 2010; Schindelka et al., 2013). Isoprene  
441 NOSs generally increased with the increasing of isoprene oxidation products (MVK+MACR) and acidic sulfate aerosols  
442 (Figs. 3 and 7, Table S4). It indicates isoprene NOSs form via acid-catalyzed reactions or reactive uptake of oxidation  
443 products of isoprene by sulfate, rather than  $\text{NO}_3$ -initiated oxidation pathways. The highest concentrations of isoprene OSs  
444 and NOSs were observed during the nighttime of May 30 during episode III (Fig. 7), with high sulfate, MVK+MACR,  
445 aerosol acidity and LWC (Fig. 3, Table S5). In the formation of isoprene OSs or NOSs, epoxides first form carbocation  
446 intermediates through acid-catalyzed hydrolysis reactions, and then sulfate ions serve as nucleophiles in the subsequent fast  
447 step forming OSs or NOSs (Minerath and Elrod, 2009). The presence of high levels of sulfate may effectively facilitate the  
448 ring-opening reaction of epoxide or reactive uptake of oxidation products and subsequent OSs or NOS formation (Surratt et  
449 al., 2010). The proposed formation mechanisms of isoprene NOSs are needed to be further investigated and validated  
450 through laboratory studies.

451 Although the isoprene NOS formation was not via the  $\text{NO}_3$ -initiated oxidation pathways, the  $\text{NO}_3$  radical could be  
452 involved in the formation pathways and influence the yield of isoprene NOSs. Considering the different atmospheric  
453 conditions during the daytime and nighttime, we analyzed the variation of daytime and nighttime isoprene NOSs separately  
454 (Fig. 8). Generally, higher concentrations of isoprene NOSs were found with elevated  $\text{NO}_2$  or MVK+MACR concentration  
455 levels. During daytime, the correlation of isoprene NOSs with  $\text{NO}_2$  ( $r=0.74$ ) was stronger than that with MVK+MACR  
456 ( $r=0.69$ ) (Fig. 8). When MVK+MACR was higher than 0.7 ppb, the NOS concentrations did not increase further with  
457 MVK+MACR. It was likely that the biogenic VOCs precursors were in surplus under this condition and the formation of  
458 isoprene NOSs may be limited by the lower daytime  $\text{NO}_2$  concentration, sulfate aerosols or other factors. During daytime,  
459 the MVK+MACR concentrations were generally higher and  $\text{NO}_x$  was lower (Fig. S5), thus the  $\text{NO}_2$  level may limit the  
460 daytime formation of isoprene NOSs. During nighttime, a strong correlation between isoprene NOS and MVK+MACR  
461 ( $r=0.94$ ) was observed, while the increase trend of isoprene NOSs as a function of  $\text{NO}_2$  ( $r=0.53$ ) was not so obvious and their  
462 correlation was lower (Fig. 8). During nighttime, the  $\text{NO}_x$  concentrations were generally higher and MVK+MACR

463 concentrations were lower (Fig. S5), thus the concentrations of isoprene oxidation products (e.g. MVK+MACR) may be the  
464 limiting factor for the nighttime formation of isoprene NOSs. The threshold (e.g.  $\text{NO}_x$ /isoprene ratio,  $\text{NO}_x$ /isoprene oxidation  
465 products ratio) that makes the transition from  $\text{NO}_x$ -limited to isoprene-limited (or isoprene oxidation products) still need  
466 further investigation through laboratory studies.

#### 467 **4 Conclusions**

468 An intensive field campaign was conducted to investigate the characterization and formation of OSs and NOSs in  
469 summer of Beijing, under the influence of abundant biogenic emissions and anthropogenic pollutants (e.g.  $\text{NO}_x$ ,  $\text{SO}_2$  and  
470  $\text{SO}_4^{2-}$ ). The overall molecular characterization of S-containing organics (CHOS, CHONS) was made through ESI-Orbitrap  
471 MS data. More than 90% of the CHOS formulas could be assigned as OSs and more than half of the CHONS formulas could  
472 be assigned as NOSs, based on the molecular formulas. The number and intensity of OSs and NOSs increased significantly  
473 during pollution episodes, which indicated they might play important roles for the SOA accumulation.

474 To further investigate the distribution and formation pathways of OSs and NOSs in complex ambient atmosphere, some  
475 species were quantified using HPLC-MS, including ten OSs and three NOS species. The total concentrations of quantified  
476 OSs and NOSs were 41.4 and 13.8  $\text{ng}/\text{m}^3$ , respectively, accounting for 0.31% and 0.11% of organic matter. Glycolic acid  
477 sulfate was the most abundant species (19.5  $\text{ng}/\text{m}^3$ ) among all the quantified OS species. The strong correlations between  
478 GAS, LAS, HAS and isoprene OSs indicated their potential formation pathways via isoprene oxidation in the presence of  
479 acidic sulfate aerosols. The concentration of isoprene OSs was 14.8  $\text{ng}/\text{m}^3$  and the isoprene OSs formed via  $\text{HO}_2$  channel was  
480 higher than that via  $\text{NO}/\text{NO}_2$  channel. The contribution of monoterpene OSs was much smaller than other OSs, while the  
481 monoterpene NOSs ( $\text{C}_{10}\text{H}_{16}\text{NO}_7\text{S}^-$ ) were observed at high concentration (12.0  $\text{ng}/\text{m}^3$ ), especially in nighttime samples.

482 OS concentrations generally increased with the increase of acidic sulfate aerosols, aerosol acidity and LWC, indicating  
483 the acid-catalyzed aqueous-phase formation of OSs in the presence of acidic sulfate aerosols as an effective formation  
484 pathway. The sulfate concentration, SIA composition, aerosol acidity, and LWC are important factors influencing the OS  
485 formation. When sulfate dominated the SIAs accumulation ( $\text{SO}_4^{2-}/\text{SIAs} > 0.5$ ), the aerosol acidity would increase obviously

486 as a function of  $\text{SO}_4^{2-}$ /SIAs mass concentration ratios and the pH values were generally below 2.8. Thus, the OS formation  
487 would be obviously promoted as the increasing of acidic sulfate aerosols, aerosol acidity and LWC. When the SIAs  
488 accumulation were dominated by nitrate ( $\text{SO}_4^{2-}$ /SIAs < 0.5), high aerosol LWC may occur, while the OS formation via  
489 acid-catalyzed reactions may be limited by relatively lower aerosol acidity.

490 The  $\text{NO}_3$ -initiated oxidation dominated the nighttime BVOCs loss in summertime Beijing, with the  $\text{NO}_x$ /BVOCs ratios  
491 higher than 10 at night. Significant nighttime enhancement of monoterpene NOSs was observed, indicating the formation via  
492  $\text{NO}_3$ -initiated oxidation of monoterpene under high- $\text{NO}_x$  conditions. Higher concentrations of monoterpene NOSs were  
493 found with elevated  $\text{NO}_2$  levels at night and  $\text{NO}_2$  ceased to be a limiting factor for NOS formation when higher than 20 ppb.  
494 The lower daytime concentrations of monoterpene NOSs could be attributed to the lower production and the decomposition  
495 during daytime. Different from the monoterpene NOS formation via  $\text{NO}_3$ -initiated oxidation, isoprene NOSs and OSs are  
496 supposed to form via acid-catalyzed chemistry or reactive uptake of the oxidation products of isoprene, which is needed to  
497 be further investigated through laboratory studies. The daytime  $\text{NO}_2$  concentration could be a limiting factor for isoprene  
498 NOS formation, while the nighttime formation was limited by isoprene or its oxidation products. The proposed formation  
499 mechanisms of isoprene NOSs as well as the limiting factors still need further investigation in laboratory studies.

500 This study highlights the formation of OSs and NOSs via the interaction between biogenic VOC precursors and  
501 anthropogenic pollutants ( $\text{NO}_x$ ,  $\text{SO}_2$  and  $\text{SO}_4^{2-}$ ) in summer of Beijing. Our study reveals the accumulation of OSs with the  
502 increase of acidic sulfate aerosols and the nighttime enhancement of monoterpene NOSs under high- $\text{NO}_x$  conditions. The  
503 acidic sulfate aerosols and high nighttime  $\text{NO}_x$  or  $\text{N}_2\text{O}_5$  concentrations were observed in Beijing in our observation and also  
504 other studies (Liu et al., 2017; Wang et al., 2017b; Wang et al., 2017a), which provide favorable conditions for the formation  
505 of OSs and NOSs. The results imply the importance of reducing anthropogenic emissions, especially  $\text{NO}_x$  and  $\text{SO}_2$ , to reduce  
506 the biogenic SOA burden in Beijing, and also in areas with abundant biogenic emissions and anthropogenic pollutants.  
507 Moreover, the OSs or NOSs could be treated as key SOA species when exploring the biogenic-anthropogenic interactions as  
508 well as organic-inorganic reactions.

509

510 *Data availability.* The dataset is available upon request by contacting Min Hu (minhu@pku.edu.cn).

511

512 **The Supplement related to this article is available online**

513

514 *Competing interests.* The authors declare that they have no conflict of interest.

515

516 *Acknowledgements.* This work was supported by National Natural Science Foundation of China (91544214, 41421064,  
517 51636003); National research program for key issues in air pollution control (DQGG0103); National Key Research and  
518 Development Program of China (2016YFC0202000: Task 3); bilateral Sweden-China framework program on  
519 ‘Photochemical smog in China: formation, transformation, impact and abatement strategies’ (639-2013-6917).

520

## 521 **References**

522 Agarwal, S., Aggarwal, S. G., Okuzawa, K., and Kawamura, K.: Size distributions of dicarboxylic acids, ketoacids,  
523  $\alpha$ -dicarbonyls, sugars, WSOC, OC, EC and inorganic ions in atmospheric particles over Northern Japan: implication for  
524 long-range transport of Siberian biomass burning and East Asian polluted aerosols, *Atmos. Chem. Phys.*, 10, 5839-5858,  
525 10.5194/acp-10-5839-2010, 2010.

526 Atkinson, R., Baulch, D. L., Cox, R. A., Crowley, J. N., Hampson, R. F., Hynes, R. G., Jenkin, M. E., Rossi, M. J., Troe, J.,  
527 and Subcommittee, I.: Evaluated kinetic and photochemical data for atmospheric chemistry: Volume II - gas phase reactions  
528 of organic species, *Atmos. Chem. Phys.*, 6, 3625-4055, 10.5194/acp-6-3625-2006, 2006.

529 Bikkina, S., Kawamura, K., and Sarin, M.: Secondary Organic Aerosol Formation over Coastal Ocean: Inferences from  
530 Atmospheric Water-Soluble Low Molecular Weight Organic Compounds, *Environ. Sci. Technol.*, 51, 4347-4357,  
531 10.1021/acs.est.6b05986, 2017.

532 Blair, S. L., MacMillan, A. C., Drozd, G. T., Goldstein, A. H., Chu, R. K., Pasa-Tolic, L., Shaw, J. B., Tolic, N., Lin, P.,  
533 Laskin, J., Laskin, A., and Nizkorodov, S. A.: Molecular Characterization of Organosulfur Compounds in Biodiesel and  
534 Diesel Fuel Secondary Organic Aerosol, *Environ. Sci. Technol.*, 51, 119-127, 10.1021/acs.est.6b03304, 2017.

535 Booth, A. M., Murphy, B., Riipinen, I., Percival, C. J., and Topping, D. O.: Connecting bulk viscosity measurements to  
536 kinetic limitations on attaining equilibrium for a model aerosol composition, *Environ. Sci. Technol.*, 48, 9298-9305,  
537 10.1021/es501705c, 2014.

538 Boreddy, S. K. R., Kawamura, K., and Tachibana, E.: Long-term (2001-2013) observations of water-soluble dicarboxylic  
539 acids and related compounds over the western North Pacific: trends, seasonality and source apportionment, *Scientific reports*,  
540 7, 8518, 10.1038/s41598-017-08745-w, 2017.

541 Brüggemann, M., Poulain, L., Held, A., Stelzer, T., Zuth, C., Richters, S., Mutzel, A., van Pinxteren, D., Iinuma, Y.,  
542 Katkevica, S., Rabe, R., Herrmann, H., and Hoffmann, T.: Real-time detection of highly oxidized organosulfates and BSOA  
543 marker compounds during the F-BEACH 2014 field study, *Atmos. Chem. Phys.*, 17, 1453-1469, 10.5194/acp-17-1453-2017,  
544 2017.

545 Budisulistiorini, S. H., Li, X., Bairai, S. T., Renfro, J., Liu, Y., Liu, Y. J., McKinney, K. A., Martin, S. T., McNeill, V. F., Pye,  
546 H. O. T., Nenes, A., Neff, M. E., Stone, E. A., Mueller, S., Knote, C., Shaw, S. L., Zhang, Z., Gold, A., and Surratt, J. D.:  
547 Examining the effects of anthropogenic emissions on isoprene-derived secondary organic aerosol formation during the 2013  
548 Southern Oxidant and Aerosol Study (SOAS) at the Look Rock, Tennessee ground site, *Atmos. Chem. Phys.*, 15, 8871-8888,  
549 10.5194/acp-15-8871-2015, 2015.

550 Carlton, A. G., Wiedinmyer, C., and Kroll, J. H.: A review of Secondary Organic Aerosol (SOA) formation from isoprene,  
551 *Atmos. Chem. Phys.*, 9, 4987-5005, 10.5194/acp-9-4987-2009, 2009.

552 Chan, M. N., and Chan, C. K.: Mass transfer effects in hygroscopic measurements of aerosol particles, *Atmos. Chem. Phys.*,  
553 5, 2703-2712, 10.5194/acp-5-2703-2005, 2005.

554 Chan, M. N., Surratt, J. D., Claeys, M., Edgerton, E. S., Tanner, R. L., Shaw, S. L., Zheng, M., Knipping, E. M., Eddingsaas,  
555 N. C., Wennberg, P. O., and Seinfeld, J. H.: Characterization and quantification of isoprene-derived epoxydiols in ambient  
556 aerosol in the southeastern United States, *Environ. Sci. Technol.*, 44, 4590-4596, 10.1021/es100596b, 2010.

557 Chan, M. N., Surratt, J. D., Chan, A. W. H., Schilling, K., Offenberg, J. H., Lewandowski, M., Edney, E. O., Kleindienst, T.  
558 E., Jaoui, M., Edgerton, E. S., Tanner, R. L., Shaw, S. L., Zheng, M., Knipping, E. M., and Seinfeld, J. H.: Influence of  
559 aerosol acidity on the chemical composition of secondary organic aerosol from  $\beta$ -caryophyllene, *Atmos. Chem. Phys.*, 11,  
560 1735-1751, 10.5194/acp-11-1735-2011, 2011.

561 Charbouillot, T., Gorini, S., Voyard, G., Parazols, M., Brigante, M., Deguillaume, L., Delort, A.-M., and Mailhot, G.:  
562 Mechanism of carboxylic acid photooxidation in atmospheric aqueous phase: Formation, fate and reactivity, *Atmos. Environ.*,  
563 56, 1-8, 10.1016/j.atmosenv.2012.03.079, 2012.

564 Chebbi, A., and Carlier, P.: Carboxylic acids in the troposphere, occurrence, sources, and sinks: A review, *Atmos. Environ.*,  
565 30, 4233-4249, 10.1016/1352-2310(96)00102-1, 1996.

566 Darer, A. I., Cole-Filipiak, N. C., O'Connor, A. E., and Elrod, M. J.: Formation and stability of atmospherically relevant  
567 isoprene-derived organosulfates and organonitrates, *Environ. Sci. Technol.*, 45, 1895-1902, 10.1021/es103797z, 2011.

568 Deshmukh, D. K., Kawamura, K., Deb, M. K., and Boreddy, S. K. R.: Sources and formation processes of water-soluble  
569 dicarboxylic acids,  $\omega$ -oxocarboxylic acids,  $\alpha$ -dicarbonyls, and major ions in summer aerosols from eastern central India, *J.*  
570 *Geophys. Res.*, [Atmos.], 122, 3630-3652, 10.1002/2016jd026246, 2017.

571 Duporte, G., Flaud, P. M., Geneste, E., Augagneur, S., Pangui, E., Lamkaddam, H., Gratien, A., Doussin, J. F., Budzinski, H.,  
572 Villenave, E., and Perraudin, E.: Experimental Study of the Formation of Organosulfates from  $\alpha$ -Pinene Oxidation. Part I:  
573 Product Identification, Formation Mechanisms and Effect of Relative Humidity, *The journal of physical chemistry. A*, 120,  
574 7909-7923, 10.1021/acs.jpca.6b08504, 2016.

575 Edwards, P. M., Aikin, K. C., Dube, W. P., Fry, J. L., Gilman, J. B., de Gouw, J. A., Graus, M. G., Hanisco, T. F., Holloway,  
576 J., Huber, G., Kaiser, J., Keutsch, F. N., Lerner, B. M., Neuman, J. A., Parrish, D. D., Peischl, J., Pollack, I. B., Ravishankara,  
577 A. R., Roberts, J. M., Ryerson, T. B., Trainer, M., Veres, P. R., Wolfe, G. M., Warneke, C., and Brown, S. S.: Transition from

578 high- to low-NO<sub>x</sub> control of night-time oxidation in the southeastern US, *Nature Geosci.*, 10, 490-495, 10.1038/NGEO2976,  
579 2017.

580 Frossard, A. A., Shaw, P. M., Russell, L. M., Kroll, J. H., Canagaratna, M. R., Worsnop, D. R., Quinn, P. K., and Bates, T. S.:  
581 Springtime Arctic haze contributions of submicron organic particles from European and Asian combustion sources, *J.*  
582 *Geophys. Res.*, [Atmos.], 116, Artn D0520510.1029/2010jd015178, 2011.

583 Froyd, K. D., Murphy, S. M., Murphy, D. M., de Gouw, J. A., Eddingsaas, N. C., and Wennberg, P. O.: Contribution of  
584 isoprene-derived organosulfates to free tropospheric aerosol mass, *Proc. Natl. Acad. Sci. USA*, 107, 21360-21365,  
585 10.1073/pnas.1012561107, 2010.

586 Fu, T.-M., Jacob, D. J., Wittrock, F., Burrows, J. P., Vrekoussis, M., and Henze, D. K.: Global budgets of atmospheric  
587 glyoxal and methylglyoxal, and implications for formation of secondary organic aerosols, *J. Geophys. Res.*, 113,  
588 10.1029/2007jd009505, 2008.

589 [Gao, S., Surratt, J. D., Knipping, E. M., Edgerton, E. S., Shahgholi, M., and Seinfeld, J. H.: Characterization of polar organic](#)  
590 [components in fine aerosols in the southeastern United States: Identity, origin, and evolution, \*J. Geophys. Res.\*, 111,](#)  
591 [10.1029/2005jd006601, 2006.](#)

592 Gómez-González, Y., Wang, W., Vermeylen, R., Chi, X., Neiryneck, J., Janssens, I. A., Maenhaut, W., and Claeys, M.:  
593 Chemical characterisation of atmospheric aerosols during a 2007 summer field campaign at Brasschaat, Belgium: sources  
594 and source processes of biogenic secondary organic aerosol, *Atmos. Chem. Phys.*, 12, 125-138, 10.5194/acp-12-125-2012,  
595 2012.

596 Gomez-Gonzalez, Y., Surratt, J. D., Cuyckens, F., Szmigielski, R., Vermeylen, R., Jaoui, M., Lewandowski, M., Offenberg, J.  
597 H., Kleindienst, T. E., Edney, E. O., Blockhuys, F., Van Alsenoy, C., Maenhaut, W., and Claeys, M.: Characterization of  
598 organosulfates from the photooxidation of isoprene and unsaturated fatty acids in ambient aerosol using liquid  
599 chromatography/(-) electrospray ionization mass spectrometry, *J. Mass Spectrom.*, 43, 371-382, 10.1002/jms.1329, 2008.

600 Guo, H., Xu, L., Bougiatioti, A., Cerully, K. M., Capps, S. L., Hite, J. R., Carlton, A. G., Lee, S. H., Bergin, M. H., Ng, N. L.,  
601 Nenes, A., and Weber, R. J.: Fine-particle water and pH in the southeastern United States, *Atmos. Chem. Phys.*, 15,  
602 5211-5228, 10.5194/acp-15-5211-2015, 2015.

603 Guo, H., Sullivan, A. P., Campuzano-Jost, P., Schroder, J. C., Lopez-Hilfiker, F. D., Dibb, J. E., Jimenez, J. L., Thornton, J.  
604 A., Brown, S. S., Nenes, A., and Weber, R. J.: Particle pH and the Partitioning of Nitric Acid during Winter in the  
605 Northeastern United States, *J. Geophys. Res.*, [Atmos.], 121, 10355-10376, 10.1002/2016JD025311, 2016.

606 Guo, S., Hu, M., Wang, Z. B., Slanina, J., and Zhao, Y. L.: Size-resolved aerosol water-soluble ionic compositions in the  
607 summer of Beijing: implication of regional secondary formation, *Atmos. Chem. Phys.*, 10, 947-959,  
608 10.5194/acp-10-947-2010, 2010.

609 Guo, S., Hu, M., Zamora, M. L., Peng, J., Shang, D., Zheng, J., Du, Z., Wu, Z., Shao, M., Zeng, L., Molina, M. J., and Zhang,  
610 R.: Elucidating severe urban haze formation in China, *Proc. Natl. Acad. Sci. USA*, 111, 17373-17378,  
611 10.1073/pnas.1419604111, 2014.

612 Hallquist, M., Wenger, J. C., Baltensperger, U., Rudich, Y., Simpson, D., Claeys, M., Dommen, J., Donahue, N. M., George,  
613 C., Goldstein, A. H., Hamilton, J. F., Herrmann, H., Hoffmann, T., Iinuma, Y., Jang, M., Jenkin, M. E., Jimenez, J. L.,  
614 Kiendler-Scharr, A., Maenhaut, W., McFiggans, G., Mentel, T. F., Monod, A., Prevot, A. S. H., Seinfeld, J. H., Surratt, J. D.,

615 Szmigielski, R., and Wildt, J.: The formation, properties and impact of secondary organic aerosol: current and emerging  
616 issues, *Atmos. Chem. Phys.*, 9, 5155-5236, 10.5194/acp-9-5155-2009, 2009.

617 Hallquist, M., Munthe, J., Hu, M., Wang, T., Chan, C. K., Gao, J., Boman, J., Guo, S., Hallquist, A. M., Mellqvist, J.,  
618 Moldanova, J., Pathak, R. K., Pettersson, J. B. C., Pleijel, H., Simpson, D., and Thynell, M.: Photochemical smog in China:  
619 scientific challenges and implications for air-quality policies, *Natl. Sci. Rev.*, 3, 401-403, 10.1093/nsr/nww080, 2016.

620 Hatch, L. E., Creamean, J. M., Ault, A. P., Surratt, J. D., Chan, M. N., Seinfeld, J. H., Edgerton, E. S., Su, Y., and Prather, K.  
621 A.: Measurements of isoprene-derived organosulfates in ambient aerosols by aerosol time-of-flight mass spectrometry-part 2:  
622 temporal variability and formation mechanisms, *Environ. Sci. Technol.*, 45, 8648-8655, 10.1021/es2011836, 2011.

623 Hawkins, L. N., Russell, L. M., Covert, D. S., Quinn, P. K., and Bates, T. S.: Carboxylic acids, sulfates, and organosulfates in  
624 processed continental organic aerosol over the southeast Pacific Ocean during VOCALS-REx 2008, *J. Geophys. Res.*,  
625 [Atmos.], 115, D13201, 10.1029/2009jd013276, 2010.

626 He, Q. F., Ding, X., Wang, X. M., Yu, J. Z., Fu, X. X., Liu, T. Y., Zhang, Z., Xue, J., Chen, D. H., Zhong, L. J., and Donahue,  
627 N. M.: Organosulfates from pinene and isoprene over the Pearl River Delta, South China: seasonal variation and implication  
628 in formation mechanisms, *Environ. Sci. Technol.*, 48, 9236-9245, 10.1021/es501299v, 2014.

629 He, S., Chen, Z., and Zhang, X.: Photochemical reactions of methyl and ethyl nitrate: a dual role for alkyl nitrates in the  
630 nitrogen cycle, *Environ. Chem.*, 8, 529, 10.1071/en10004, 2011.

631 Hennigan, C. J., Izumi, J., Sullivan, A. P., Weber, R. J., and Nenes, A.: A critical evaluation of proxy methods used to  
632 estimate the acidity of atmospheric particles, *Atmos. Chem. Phys.*, 15, 2775-2790, 10.5194/acp-15-2775-2015, 2015.

633 Herndon, S. C., Onasch, T. B., Wood, E. C., Kroll, J. H., Canagaratna, M. R., Jayne, J. T., Zavala, M. A., Knighton, W. B.,  
634 Mazzoleni, C., Dubey, M. K., Ulbrich, I. M., Jimenez, J. L., Seila, R., de Gouw, J. A., de Foy, B., Fast, J., Molina, L. T., Kolb,  
635 C. E., and Worsnop, D. R.: Correlation of secondary organic aerosol with odd oxygen in Mexico City, *Geophys. Res. Lett.*,  
636 35, 10.1029/2008gl034058, 2008.

637 Hettiyadura, A. P. S., Stone, E. A., Kundu, S., Baker, Z., Geddes, E., Richards, K., and Humphry, T.: Determination of  
638 atmospheric organosulfates using HILIC chromatography with MS detection, *Atmos. Meas. Tech.*, 8, 2347-2358,  
639 10.5194/amt-8-2347-2015, 2015.

640 Hettiyadura, A. P. S., Jayarathne, T., Baumann, K., Goldstein, A. H., de Gouw, J. A., Koss, A., Keutsch, F. N., Skog, K., and  
641 Stone, E. A.: Qualitative and quantitative analysis of atmospheric organosulfates in Centreville, Alabama, *Atmos. Chem.*  
642 *Phys.*, 17, 1343-1359, 10.5194/acp-17-1343-2017, 2017.

643 Hu, K. S., Darer, A. I., and Elrod, M. J.: Thermodynamics and kinetics of the hydrolysis of atmospherically relevant  
644 organonitrates and organosulfates, *Atmos. Chem. Phys.*, 11, 8307-8320, 10.5194/acp-11-8307-2011, 2011.

645 Hu, W. W., Campuzano-Jost, P., Palm, B. B., Day, D. A., Ortega, A. M., Hayes, P. L., Krechmer, J. E., Chen, Q., Kuwata, M.,  
646 Liu, Y. J., de S á S. S., McKinney, K., Martin, S. T., Hu, M., Budisulistiorini, S. H., Riva, M., Surratt, J. D., St. Clair, J. M.,  
647 Isaacman-Van Wertz, G., Yee, L. D., Goldstein, A. H., Carbone, S., Brito, J., Artaxo, P., de Gouw, J. A., Koss, A., Wisthaler,  
648 A., Mikoviny, T., Karl, T., Kaser, L., Jud, W., Hansel, A., Docherty, K. S., Alexander, M. L., Robinson, N. H., Coe, H., Allan,  
649 J. D., Canagaratna, M. R., Paulot, F., and Jimenez, J. L.: Characterization of a real-time tracer for isoprene  
650 epoxydiols-derived secondary organic aerosol (IEPOX-SOA) from aerosol mass spectrometer measurements, *Atmos. Chem.*  
651 *Phys.*, 15, 11807-11833, 10.5194/acp-15-11807-2015, 2015.

652 Iinuma, Y., Muller, C., Berndt, T., Boge, O., Claeys, M., and Herrmann, H.: Evidence for the existence of organosulfates  
653 from  $\beta$ -pinene ozonolysis in ambient secondary organic aerosol, *Environ. Sci. Technol.*, 41, 6678-6683, 10.1021/es070938t,  
654 2007.

655 Jimenez, J. L., Canagaratna, M. R., Donahue, N. M., Prevot, A. S., Zhang, Q., Kroll, J. H., DeCarlo, P. F., Allan, J. D., Coe,  
656 H., Ng, N. L., Aiken, A. C., Docherty, K. S., Ulbrich, I. M., Grieshop, A. P., Robinson, A. L., Duplissy, J., Smith, J. D.,  
657 Wilson, K. R., Lanz, V. A., Hueglin, C., Sun, Y. L., Tian, J., Laaksonen, A., Raatikainen, T., Rautiainen, J., Vaattovaara, P.,  
658 Ehn, M., Kulmala, M., Tomlinson, J. M., Collins, D. R., Cubison, M. J., Dunlea, E. J., Huffman, J. A., Onasch, T. B., Alfarra,  
659 M. R., Williams, P. I., Bower, K., Kondo, Y., Schneider, J., Drewnick, F., Borrmann, S., Weimer, S., Demerjian, K., Salcedo,  
660 D., Cottrell, L., Griffin, R., Takami, A., Miyoshi, T., Hatakeyama, S., Shimono, A., Sun, J. Y., Zhang, Y. M., Dzepina, K.,  
661 Kimmel, J. R., Sueper, D., Jayne, J. T., Herndon, S. C., Trimborn, A. M., Williams, L. R., Wood, E. C., Middlebrook, A. M.,  
662 Kolb, C. E., Baltensperger, U., and Worsnop, D. R.: Evolution of organic aerosols in the atmosphere, *Science*, 326,  
663 1525-1529, 10.1126/science.1180353, 2009.

664 Kawamura, K., Kasukabe, H., and Barrie, L. A.: Secondary formation of water-soluble organic acids and  $\alpha$ -dicarbonyls and  
665 their contributions to total carbon and water-soluble organic carbon: Photochemical aging of organic aerosols in the Arctic  
666 spring, *J. Geophys. Res.*, 115, 10.1029/2010jd014299, 2010.

667 Kiehl, J. T.: Twentieth century climate model response and climate sensitivity, *Geophys. Res. Lett.*, 34,  
668 10.1029/2007gl031383, 2007.

669 Kroll, J. H., and Seinfeld, J. H.: Chemistry of secondary organic aerosol: Formation and evolution of low-volatility organics  
670 in the atmosphere, *Atmos. Environ.*, 42, 3593-3624, 10.1016/j.atmosenv.2008.01.003, 2008.

671 Lal, V., Khalizov, A. F., Lin, Y., Galvan, M. D., Connell, B. T., and Zhang, R.: Heterogeneous reactions of epoxides in acidic  
672 media, *The journal of physical chemistry. A*, 116, 6078-6090, 10.1021/jp2112704, 2012.

673 Lee, B. H., Mohr, C., Lopez-Hilfiker, F. D., Lutz, A., Hallquist, M., Lee, L., Romer, P., Cohen, R. C., Iyer, S., Kurten, T., Hu,  
674 W., Day, D. A., Campuzano-Jost, P., Jimenez, J. L., Xu, L., Ng, N. L., Guo, H., Weber, R. J., Wild, R. J., Brown, S. S., Koss,  
675 A., de Gouw, J., Olson, K., Goldstein, A. H., Seco, R., Kim, S., McAvey, K., Shepson, P. B., Starn, T., Baumann, K.,  
676 Edgerton, E. S., Liu, J., Shilling, J. E., Miller, D. O., Brune, W., Schobesberger, S., D'Ambro, E. L., and Thornton, J. A.:  
677 Highly functionalized organic nitrates in the southeast United States: Contribution to secondary organic aerosol and reactive  
678 nitrogen budgets, *Proc. Natl. Acad. Sci. USA*, 113, 1516-1521, 10.1073/pnas.1508108113, 2016.

679 Li, W., Sun, J., Xu, L., Shi, Z., Riemer, N., Sun, Y., Fu, P., Zhang, J., Lin, Y., Wang, X., Shao, L., Chen, J., Zhang, X., Wang,  
680 Z., and Wang, W.: A conceptual framework for mixing structures in individual aerosol particles, *J. Geophys. Res.*, [Atmos.],  
681 121, 13,784-713,798, 10.1002/2016jd025252, 2016.

682 Liao, J., Froyd, K. D., Murphy, D. M., Keutsch, F. N., Yu, G., Wennberg, P. O., St Clair, J. M., Crouse, J. D., Wisthaler, A.,  
683 Mikoviny, T., Jimenez, J. L., Campuzano-Jost, P., Day, D. A., Hu, W., Ryerson, T. B., Pollack, I. B., Peischl, J., Anderson, B.  
684 E., Ziemba, L. D., Blake, D. R., Meinardi, S., and Diskin, G.: Airborne measurements of organosulfates over the continental  
685 U.S, *J. Geophys. Res.*, [Atmos.], 120, 2990-3005, 10.1002/2014JD022378, 2015.

686 Liggio, J., and Li, S.-M.: Organosulfate formation during the uptake of pinonaldehyde on acidic sulfate aerosols, *Geophys.*  
687 *Res. Lett.*, 33, 10.1029/2006gl026079, 2006.

688 Lin, P., Huang, X. F., He, L. Y., and Yu, J. Z.: Abundance and size distribution of HULIS in ambient aerosols at a rural site in

689 South China, *J. Aerosol Sci.*, 41, 74-87, 10.1016/j.jaerosci.2009.09.001, 2010.

690 Lin, P., Yu, J. Z., Engling, G., and Kalberer, M.: Organosulfates in humic-like substance fraction isolated from aerosols at  
691 seven locations in East Asia: a study by ultra-high-resolution mass spectrometry, *Environ. Sci. Technol.*, 46, 13118-13127,  
692 10.1021/es303570v, 2012.

693 Lin, Y. H., Knipping, E. M., Edgerton, E. S., Shaw, S. L., and Surratt, J. D.: Investigating the influences of SO<sub>2</sub> and NH<sub>3</sub>  
694 levels on isoprene-derived secondary organic aerosol formation using conditional sampling approaches, *Atmos. Chem. Phys.*,  
695 13, 8457-8470, 10.5194/acp-13-8457-2013, 2013a.

696 Lin, Y. H., Zhang, H., Pye, H. O., Zhang, Z., Marth, W. J., Park, S., Arashiro, M., Cui, T., Budisulistiorini, S. H., Sexton, K.  
697 G., Vizuete, W., Xie, Y., Luecken, D. J., Piletic, I. R., Edney, E. O., Bartolotti, L. J., Gold, A., and Surratt, J. D.: Epoxide as a  
698 precursor to secondary organic aerosol formation from isoprene photooxidation in the presence of nitrogen oxides, *Proc. Natl.*  
699 *Acad. Sci. USA*, 110, 6718-6723, 10.1073/pnas.1221150110, 2013b.

700 Liu, M., Song, Y., Zhou, T., Xu, Z., Yan, C., Zheng, M., Wu, Z., Hu, M., Wu, Y., and Zhu, T.: Fine particle pH during severe  
701 haze episodes in northern China, *Geophys. Res. Lett.*, 44, 5213-5221, 10.1002/2017gl073210, 2017.

702 Ma, Y., Xu, X. K., Song, W. H., Geng, F. H., and Wang, L.: Seasonal and diurnal variations of particulate organosulfates in  
703 urban Shanghai, China, *Atmos. Environ.*, 85, 152-160, 10.1016/j.atmosenv.2013.12.017, 2014.

704 McNeill, V. F., Woo, J. L., Kim, D. D., Schwier, A. N., Wannell, N. J., Sumner, A. J., and Barakat, J. M.: Aqueous-phase  
705 secondary organic aerosol and organosulfate formation in atmospheric aerosols: a modeling study, *Environ. Sci. Technol.*, 46,  
706 8075-8081, 10.1021/es3002986, 2012.

707 McNeill, V. F.: Aqueous organic chemistry in the atmosphere: sources and chemical processing of organic aerosols, *Environ.*  
708 *Sci. Technol.*, 49, 1237-1244, 10.1021/es5043707, 2015.

709 Meade, L. E., Riva, M., Blomberg, M. Z., Brock, A. K., Qualters, E. M., Siejack, R. A., Ramakrishnan, K., Surratt, J. D., and  
710 Kautzman, K. E.: Seasonal variations of fine particulate organosulfates derived from biogenic and anthropogenic  
711 hydrocarbons in the mid-Atlantic United States, *Atmos. Environ.*, 145, 405-414, 10.1016/j.atmosenv.2016.09.028, 2016.

712 Minerath, E. C., Casale, M. T., and Elrod, M. J.: Kinetics Feasibility Study of Alcohol Sulfate Esterification Reactions in  
713 Tropospheric Aerosols, *Environ. Sci. Technol.*, 42, 4410-4415, 10.1021/es8004333, 2008.

714 Minerath, E. C., and Elrod, M. J.: Assessing the potential for diol and hydroxy sulfate ester formation from the reaction of  
715 epoxides in tropospheric aerosols, *Environ. Sci. Technol.*, 43, 1386-1392, 10.1021/es8029076, 2009.

716 Narukawa, M.: Fine and coarse modes of dicarboxylic acids in the Arctic aerosols collected during the Polar Sunrise  
717 Experiment 1997, *J. Geophys. Res.*, 108, 10.1029/2003jd003646, 2003.

718 Nguyen, T. B., Bates, K. H., Crouse, J. D., Schwantes, R. H., Zhang, X., Kjaergaard, H. G., Surratt, J. D., Lin, P., Laskin, A.,  
719 Seinfeld, J. H., and Wennberg, P. O.: Mechanism of the hydroxyl radical oxidation of methacryloyl peroxyxynitrate (MPAN)  
720 and its pathway toward secondary organic aerosol formation in the atmosphere, *Phys. Chem. Chem. Phys.*, 17, 17914-17926,  
721 10.1039/c5cp02001h, 2015.

722 Nozière, B., Ekström, S., Alsberg, T., and Holmström, S.: Radical-initiated formation of organosulfates and surfactants in  
723 atmospheric aerosols, *Geophys. Res. Lett.*, 37, 10.1029/2009gl041683, 2010.

724 Olson, C. N., Galloway, M. M., Yu, G., Hedman, C. J., Lockett, M. R., Yoon, T., Stone, E. A., Smith, L. M., and Keutsch, F.  
725 N.: Hydroxycarboxylic acid-derived organosulfates: synthesis, stability, and quantification in ambient aerosol, *Environ. Sci.*

726 Technol., 45, 6468-6474, 10.1021/es201039p, 2011.

727 Paulot, F., Crounse, J. D., Kjaergaard, H. G., Kurten, A., St Clair, J. M., Seinfeld, J. H., and Wennberg, P. O.: Unexpected  
728 epoxide formation in the gas-phase photooxidation of isoprene, *Science*, 325, 730-733, 10.1126/science.1172910, 2009.

729 Rattanavaraha, W., Chu, K., Budisulistiorini, S. H., Riva, M., Lin, Y.-H., Edgerton, E. S., Baumann, K., Shaw, S. L., Guo, H.,  
730 King, L., Weber, R. J., Neff, M. E., Stone, E. A., Offenberg, J. H., Zhang, Z., Gold, A., and Surratt, J. D.: Assessing the  
731 impact of anthropogenic pollution on isoprene-derived secondary organic aerosol formation in PM<sub>2.5</sub> collected from the  
732 Birmingham, Alabama, ground site during the 2013 Southern Oxidant and Aerosol Study, *Atmos. Chem. Phys.*, 16,  
733 4897-4914, 10.5194/acp-16-4897-2016, 2016.

734 Renbaum-Wolff, L., Grayson, J. W., Bateman, A. P., Kuwata, M., Sellier, M., Murray, B. J., Shilling, J. E., Martin, S. T., and  
735 Bertram, A. K.: Viscosity of  $\alpha$ -pinene secondary organic material and implications for particle growth and reactivity, *Proc.*  
736 *Natl. Acad. Sci. USA*, 110, 8014-8019, 10.1073/pnas.1219548110, 2013.

737 Riedel, T. P., Lin, Y.-H., Budisulistiorini, S. H., Gaston, C. J., Thornton, J. A., Zhang, Z., Vizuete, W., Gold, A., and Surratt, J.  
738 D.: Heterogeneous Reactions of Isoprene-Derived Epoxides: Reaction Probabilities and Molar Secondary Organic Aerosol  
739 Yield Estimates, *Environmental Science & Technology Letters*, 2, 38-42, 10.1021/ez500406f, 2015.

740 Riva, M., Tomaz, S., Cui, T., Lin, Y. H., Perraudin, E., Gold, A., Stone, E. A., Villenave, E., and Surratt, J. D.: Evidence for  
741 an unrecognized secondary anthropogenic source of organosulfates and sulfonates: gas-phase oxidation of polycyclic  
742 aromatic hydrocarbons in the presence of sulfate aerosol, *Environ. Sci. Technol.*, 49, 6654-6664, 10.1021/acs.est.5b00836,  
743 2015.

744 Riva, M., Bell, D. M., Hansen, A. M., Drozd, G. T., Zhang, Z., Gold, A., Imre, D., Surratt, J. D., Glasius, M., and Zelenyuk,  
745 A.: Effect of Organic Coatings, Humidity and Aerosol Acidity on Multiphase Chemistry of Isoprene Epoxydiols, *Environ.*  
746 *Sci. Technol.*, 50, 5580-5588, 10.1021/acs.est.5b06050, 2016a.

747 Riva, M., Budisulistiorini, S. H., Zhang, Z., Gold, A., and Surratt, J. D.: Chemical characterization of secondary organic  
748 aerosol constituents from isoprene ozonolysis in the presence of acidic aerosol, *Atmos. Environ.*, 130, 5-13,  
749 10.1016/j.atmosenv.2015.06.027, 2016b.

750 Riva, M., Da Silva Barbosa, T., Lin, Y.-H., Stone, E. A., Gold, A., and Surratt, J. D.: Chemical characterization of  
751 organosulfates in secondary organic aerosol derived from the photooxidation of alkanes, *Atmos. Chem. Phys.*, 16,  
752 11001-11018, 10.5194/acp-16-11001-2016, 2016c.

753 Schindelka, J., Iinuma, Y., Hoffmann, D., and Herrmann, H.: Sulfate radical-initiated formation of isoprene-derived  
754 organosulfates in atmospheric aerosols, *Faraday Discussions*, 165, 237, 10.1039/c3fd00042g, 2013.

755 Shalamzari, M. S., Kahnt, A., Vermeylen, R., Kleindienst, T. E., Lewandowski, M., Cuyckens, F., Maenhaut, W., and Claeys,  
756 M.: Characterization of polar organosulfates in secondary organic aerosol from the green leaf volatile 3-Z-hexenal, *Environ.*  
757 *Sci. Technol.*, 48, 12671-12678, 10.1021/es503226b, 2014.

758 Shalamzari, M. S., Vermeylen, R., Blockhuys, F., Kleindienst, T. E., Lewandowski, M., Szmigielski, R., Rudzinski, K. J.,  
759 Spólnik, G., Danikiewicz, W., Maenhaut, W., and Claeys, M.: Characterization of polar organosulfates in secondary organic  
760 aerosol from the unsaturated aldehydes 2-E-pentenal, 2-E-hexenal, and 3-Z-hexenal, *Atmos. Chem. Phys.*, 16, 7135-7148,  
761 10.5194/acp-16-7135-2016, 2016.

762 Shiraiwa, M., Ammann, M., Koop, T., and Poschl, U.: Gas uptake and chemical aging of semisolid organic aerosol particles,

763 Proc. Natl. Acad. Sci. USA, 108, 11003-11008, 10.1073/pnas.1103045108, 2011.

764 Shrestha, M., Zhang, Y., Upshur, M. A., Liu, P., Blair, S. L., Wang, H. F., Nizkorodov, S. A., Thomson, R. J., Martin, S. T.,  
765 and Geiger, F. M.: On surface order and disorder of alpha-pinene-derived secondary organic material, *J. Phys. Chem. A*, 119,  
766 4609-4617, 10.1021/jp510780e, 2015.

767 Shrivastava, M., Cappa, C. D., Fan, J., Goldstein, A. H., Guenther, A. B., Jimenez, J. L., Kuang, C., Laskin, A., Martin, S. T.,  
768 Ng, N. L., Petaja, T., Pierce, J. R., Rasch, P. J., Roldin, P., Seinfeld, J. H., Shilling, J., Smith, J. N., Thornton, J. A., Volkamer,  
769 R., Wang, J., Worsnop, D. R., Zaveri, R. A., Zelenyuk, A., and Zhang, Q.: Recent advances in understanding secondary  
770 organic aerosol: Implications for global climate forcing, *Rev. Geophys.*, 55, 509-559, 10.1002/2016rg000540, 2017.

771 Staudt, S., Kundu, S., Lehmler, H. J., He, X., Cui, T., Lin, Y. H., Kristensen, K., Glasius, M., Zhang, X., Weber, R. J., Surratt,  
772 J. D., and Stone, E. A.: Aromatic organosulfates in atmospheric aerosols: synthesis, characterization, and abundance, *Atmos*  
773 *Environ* (1994), 94, 366-373, 10.1016/j.atmosenv.2014.05.049, 2014.

774 Stone, E. A., Yang, L., Yu, L. E., and Rupakheti, M.: Characterization of organosulfates in atmospheric aerosols at Four  
775 Asian locations, *Atmos. Environ.*, 47, 323-329, 10.1016/j.atmosenv.2011.10.058, 2012.

776 Suarez-Bertoa, R., Picquet-Varrault, B., Tamas, W., Pangui, E., and Doussin, J. F.: Atmospheric fate of a series of carbonyl  
777 nitrates: photolysis frequencies and OH-oxidation rate constants, *Environ. Sci. Technol.*, 46, 12502-12509,  
778 10.1021/es302613x, 2012.

779 Surratt, J. D., Kroll, J. H., Kleindienst, T. E., Edney, E. O., Claeys, M., Sorooshian, A., Ng, N. L., Offenberg, J. H.,  
780 Lewandowski, M., Jaoui, M., Flagan, R. C., and Seinfeld, J. H.: Evidence for Organosulfates in Secondary Organic Aerosol,  
781 *Environ. Sci. Technol.*, 41, 517-527, 10.1021/es062081q, 2007.

782 Surratt, J. D., Gomez-Gonzalez, Y., Chan, A. W., Vermeylen, R., Shahgholi, M., Kleindienst, T. E., Edney, E. O., Offenberg,  
783 J. H., Lewandowski, M., Jaoui, M., Maenhaut, W., Claeys, M., Flagan, R. C., and Seinfeld, J. H.: Organosulfate formation in  
784 biogenic secondary organic aerosol, *J. Phys. Chem. A*, 112, 8345-8378, 10.1021/jp802310p, 2008.

785 Surratt, J. D., Chan, A. W., Eddingsaas, N. C., Chan, M., Loza, C. L., Kwan, A. J., Hersey, S. P., Flagan, R. C., Wennberg, P.  
786 O., and Seinfeld, J. H.: Reactive intermediates revealed in secondary organic aerosol formation from isoprene, *Proc. Natl.*  
787 *Acad. Sci. USA*, 107, 6640-6645, 10.1073/pnas.0911114107, 2010.

788 Tang, R., Wu, Z., Li, X., Wang, Y., Shang, D., Xiao, Y., Li, M., Zeng, L., Wu, Z., Hallquist, M., Hu, M., and Guo, S.: Primary  
789 and secondary organic aerosols in 2016 summer of Beijing, *Atmos. Chem. Phys.*, 1-35, 10.5194/acp-2017-867, 2017.

790 Tao, S., Lu, X., Levac, N., Bateman, A. P., Nguyen, T. B., Bones, D. L., Nizkorodov, S. A., Laskin, J., Laskin, A., and Yang,  
791 X.: Molecular characterization of organosulfates in organic aerosols from Shanghai and Los Angeles urban areas by  
792 nanospray-desorption electrospray ionization high-resolution mass spectrometry, *Environ. Sci. Technol.*, 48, 10993-11001,  
793 10.1021/es5024674, 2014.

794 Tolocka, M. P., and Turpin, B.: Contribution of organosulfur compounds to organic aerosol mass, *Environ. Sci. Technol.*, 46,  
795 7978-7983, 10.1021/es300651v, 2012.

796 Turpin, B. J., and Lim, H.-J.: Species Contributions to PM<sub>2.5</sub> Mass Concentrations: Revisiting Common Assumptions for  
797 Estimating Organic Mass, *Aerosol Sci. Tech.*, 35, 602-610, 10.1080/02786820119445, 2001.

798 Vaden, T. D., Imre, D., Beranek, J., Shrivastava, M., and Zelenyuk, A.: Evaporation kinetics and phase of laboratory and  
799 ambient secondary organic aerosol, *Proc. Natl. Acad. Sci. USA*, 108, 2190-2195, 10.1073/pnas.1013391108, 2011.

800 Wang, H., Chen, J., and Lu, K.: Development of a portable cavity-enhanced absorption spectrometer for the measurement of  
801 ambient NO<sub>3</sub> and N<sub>2</sub>O<sub>5</sub>: experimental setup, lab characterizations, and field applications in a polluted urban environment,  
802 *Atmos. Meas. Tech.*, 10, 1465-1479, 10.5194/amt-10-1465-2017, 2017a.

803 Wang, H., Lu, K., Chen, X., Zhu, Q., Chen, Q., Guo, S., Jiang, M., Li, X., Shang, D., Tan, Z., Wu, Y., Wu, Z., Zou, Q., Zheng,  
804 Y., Zeng, L., Zhu, T., Hu, M., and Zhang, Y.: High N<sub>2</sub>O<sub>5</sub> Concentrations Observed in Urban Beijing: Implications of a Large  
805 Nitrate Formation Pathway, *Environmental Science & Technology Letters*, 4, 416-420, 10.1021/acs.estlett.7b00341, 2017b.

806 Wang, H., Lu, K., Guo, S., Wu, Z., Shang, D., Tan, Z., Wang, Y., Le Breton, M., Zhu, W., Lou, S., Tang, M., Wu, Y., Zheng,  
807 J., Zeng, L., Hallquist, M., Hu, M., and Zhang, Y.: Efficient N<sub>2</sub>O<sub>5</sub> Uptake and NO<sub>3</sub> Oxidation in the Outflow of Urban  
808 Beijing, *Atmos. Chem. Phys. Disc.*, 1-27, 10.5194/acp-2018-88, 2018.

809 Wang, X. K., Rossignol, S., Ma, Y., Yao, L., Wang, M. Y., Chen, J. M., George, C., and Wang, L.: Molecular characterization  
810 of atmospheric particulate organosulfates in three megacities at the middle and lower reaches of the Yangtze River, *Atmos.*  
811 *Chem. Phys.*, 16, 2285-2298, 10.5194/acp-16-2285-2016, 2016.

812 Wang, Y., Hu, M., Lin, P., Guo, Q., Wu, Z., Li, M., Zeng, L., Song, Y., Zeng, L., Wu, Y., Guo, S., Huang, X., and He, L.:  
813 Molecular Characterization of Nitrogen-Containing Organic Compounds in Humic-like Substances Emitted from Straw  
814 Residue Burning, *Environ. Sci. Technol.*, 51, 5951-5961, 10.1021/acs.est.7b00248, 2017c.

815 Wang, Y., Ren, J., Huang, X. H. H., Tong, R., and Yu, J. Z.: Synthesis of Four Monoterpene-Derived Organosulfates and  
816 Their Quantification in Atmospheric Aerosol Samples, *Environ. Sci. Technol.*, 51, 6791-6801, 10.1021/acs.est.7b01179,  
817 2017d.

818 Weber, R. J., Guo, H., Russell, A. G., and Nenes, A.: High aerosol acidity despite declining atmospheric sulfate  
819 concentrations over the past 15 years, *Nature Geosci.*, 9, 282-285, 10.1038/ngeo2665, 2016.

820 Worton, D. R., Surratt, J. D., Lafranchi, B. W., Chan, A. W., Zhao, Y., Weber, R. J., Park, J. H., Gilman, J. B., de Gouw, J.,  
821 Park, C., Schade, G., Beaver, M., Clair, J. M., Crounse, J., Wennberg, P., Wolfe, G. M., Harrold, S., Thornton, J. A., Farmer,  
822 D. K., Docherty, K. S., Cubison, M. J., Jimenez, J. L., Frossard, A. A., Russell, L. M., Kristensen, K., Glasius, M., Mao, J.,  
823 Ren, X., Brune, W., Browne, E. C., Pusede, S. E., Cohen, R. C., Seinfeld, J. H., and Goldstein, A. H.: Observational insights  
824 into aerosol formation from isoprene, *Environ. Sci. Technol.*, 47, 11403-11413, 10.1021/es4011064, 2013.

825 Wu, Z., Wang, Y., Tan, T., Zhu, Y., Li, M., Shang, D., Wang, H., Lu, K., Guo, S., Zeng, L., and Zhang, Y.: Aerosol Liquid  
826 Water Driven by Anthropogenic Inorganic Salts: Implying Its Key Role in Haze Formation over the North China Plain,  
827 *Environmental Science & Technology Letters*, 10.1021/acs.estlett.8b00021, 2018.

828 Xu L., Guo H., Boyd C. M., Klein M., Bougiatioti A., Cerully K., Hite J., Wertz G., Kreisberg N., Knote C., Olson K., Koss  
829 A., Goldstein A., Hering S., Gouw J., Baumann K., Lee S., Nenes A., Weber R., and Ng, N. L: Effects of anthropogenic  
830 emissions on aerosol formation from isoprene and monoterpenes in the southeastern United States, *Proc. Natl. Acad. Sci.*  
831 *USA*, 112, E4506-4507, 10.1073/pnas.1417609112, 2015.

832 Xue, J., Griffith, S. M., Yu, X., Lau, A. K. H., and Yu, J. Z.: Effect of nitrate and sulfate relative abundance in PM<sub>2.5</sub> on liquid  
833 water content explored through half-hourly observations of inorganic soluble aerosols at a polluted receptor site, *Atmos.*  
834 *Environ.*, 99, 24-31, 10.1016/j.atmosenv.2014.09.049, 2014.

835 Zhang, H., Worton, D. R., Lewandowski, M., Ortega, J., Rubitschun, C. L., Park, J. H., Kristensen, K., Campuzano-Jost, P.,  
836 Day, D. A., Jimenez, J. L., Jaoui, M., Offenberg, J. H., Kleindienst, T. E., Gilman, J., Kuster, W. C., de Gouw, J., Park, C.,

837 Schade, G. W., Frossard, A. A., Russell, L., Kaser, L., Jud, W., Hansel, A., Cappellin, L., Karl, T., Glasius, M., Guenther, A.,  
838 Goldstein, A. H., Seinfeld, J. H., Gold, A., Kamens, R. M., and Surratt, J. D.: Organosulfates as tracers for secondary organic  
839 aerosol (SOA) formation from 2-methyl-3-buten-2-ol (MBO) in the atmosphere, *Environ. Sci. Technol.*, 46, 9437-9446,  
840 10.1021/es301648z, 2012.

841 Zhang, Y., Chen, Y., Lambe, A. T., Olson, N. E., Lei, Z., Craig, R. L., Zhang, Z., Gold, A., Onasch, T. B., Jayne, J. T.,  
842 Worsnop, D. R., Gaston, C. J., Thornton, J. A., Vizuete, W., Ault, A. P., and Surratt, J. D.: Effect of the Aerosol-Phase State  
843 on Secondary Organic Aerosol Formation from the Reactive Uptake of Isoprene-Derived Epoxydiols (IEPOX),  
844 *Environmental Science & Technology Letters*, 5, 167-174, 10.1021/acs.estlett.8b00044, 2018.

845 Zhang, Y., Sanchez, M. S., Douet, C., Wang, Y., Bateman, A. P., Gong, Z., Kuwata, M., Renbaum-Wolff, L., Sato, B. B., Liu,  
846 P. F., Bertram, A. K., Geiger, F. M., and Martin, S. T.: Changing shapes and implied viscosities of suspended submicron  
847 particles, *Atmos. Chem. Phys.*, 15, 7819-7829, 10.5194/acp-15-7819-2015, 2015.

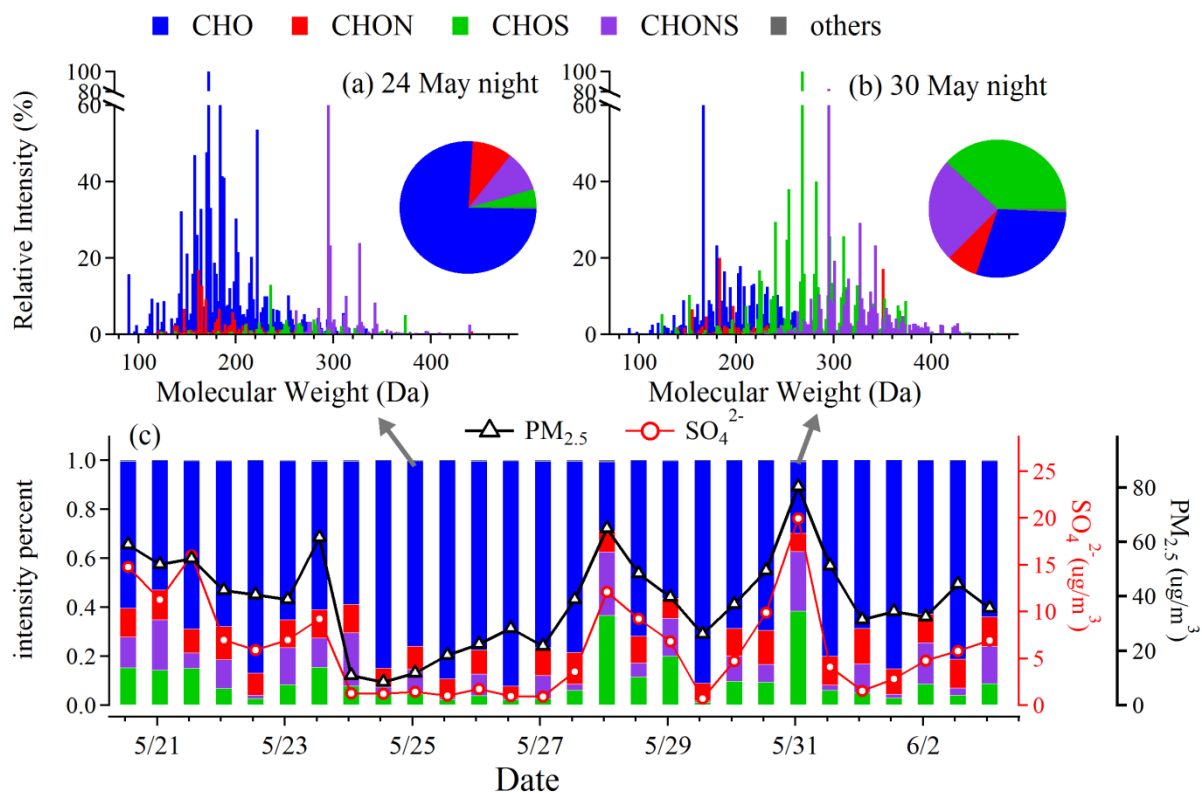
848 Zhang, Y. J., Tang, L. L., Sun, Y. L., Favez, O., Canonaco, F., Albinet, A., Couvidat, F., Liu, D. T., Jayne, J. T., Wang, Z.,  
849 Croteau, P. L., Canagaratna, M. R., Zhou, H. C., Prevot, A. S. H., and Worsnop, D. R.: Limited formation of isoprene  
850 epoxydiols-derived secondary organic aerosol under NO<sub>x</sub>-rich environments in Eastern China, *Geophys. Res. Lett.*, 44,  
851 2035-2043, 10.1002/2016GL072368, 2017.

852 Zheng, J., Hu, M., Du, Z. F., Shang, D. J., Gong, Z. H., Qin, Y. H., Fang, J. Y., Gu, F. T., Li, M. R., Peng, J. F., Li, J., Zhang,  
853 Y. Q., Huang, X. F., He, L. Y., Wu, Y. S., and Guo, S.: Influence of biomass burning from South Asia at a high-altitude  
854 mountain receptor site in China, *Atmos. Chem. Phys.*, 17, 6853-6864, 10.5194/acp-17-6853-2017, 2017.

855  
856  
857  
858  
859  
860  
861  
862  
863  
864  
865  
866  
867  
868  
869  
870  
871  
872  
873

874  
875  
876  
877  
878  
879

880 **Figures**



881

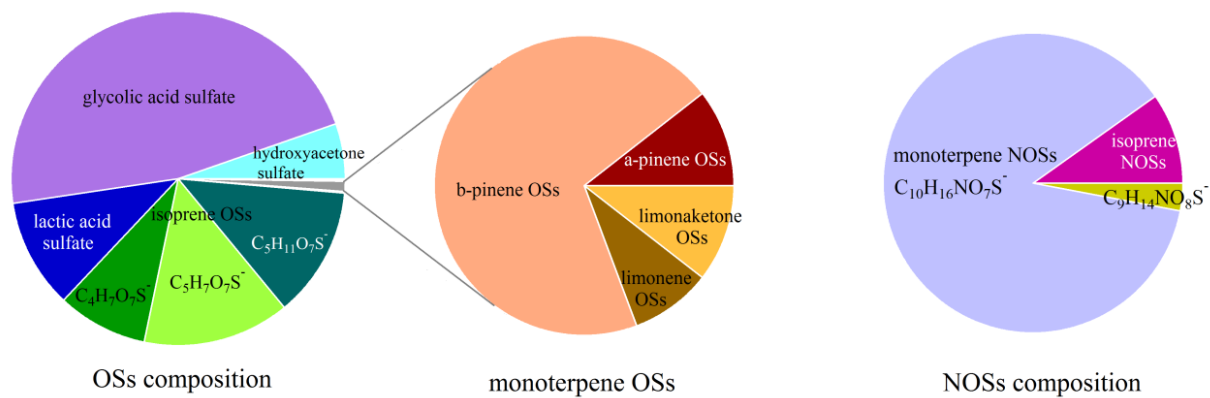
882 Figure 1 The intensity distribution of different compound categories (CHO, CHON, CHOS and CHONS) (a) on a clean day  
883 and (b) on a polluted day. (c) Temporal variation of PM<sub>2.5</sub>, SO<sub>4</sub><sup>2-</sup> and intensity percentages of different compound categories.  
884 The highly water-soluble OS species (e.g. isoprene OSs) with lower MW are absent in these figures and details are described  
885 in section 3.1.

886

887

888

889



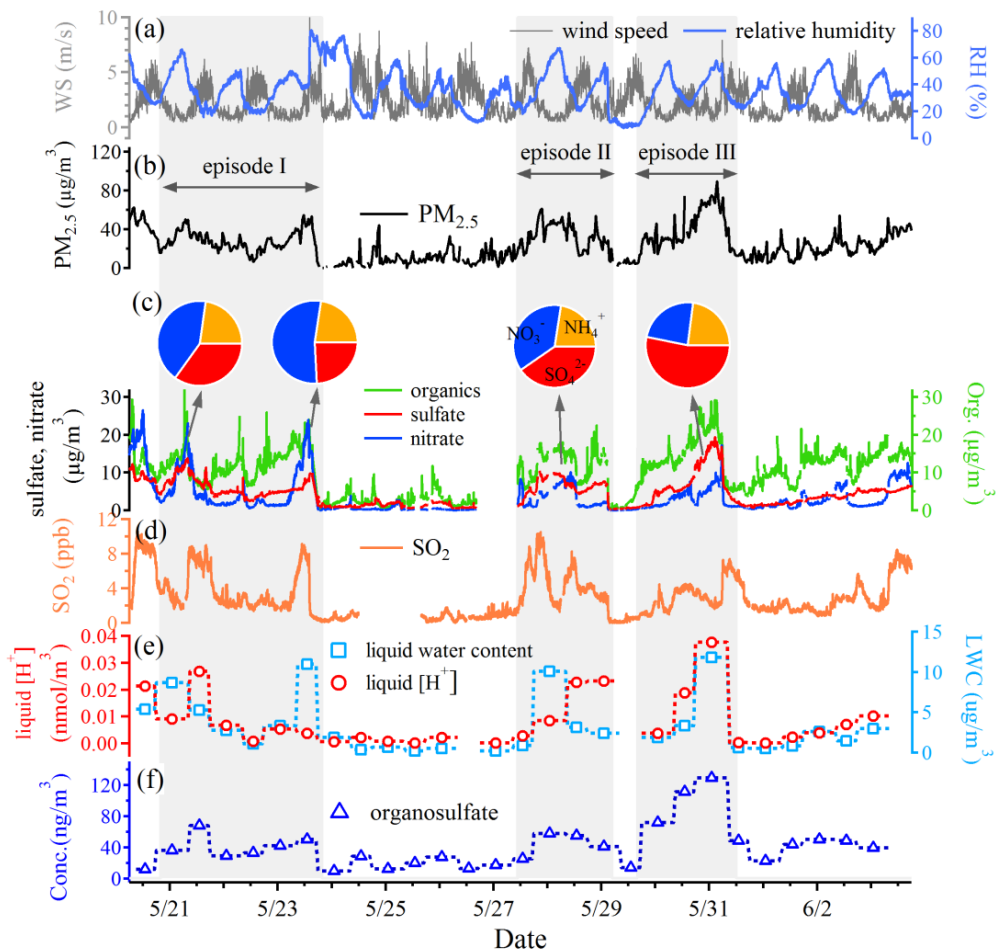
890

891 Figure 2 The relative contribution of different OS and NOS species. Only the selected species (semi-)quantified by  
892 HPLC-MS are included in this figure.

893

894

895



896

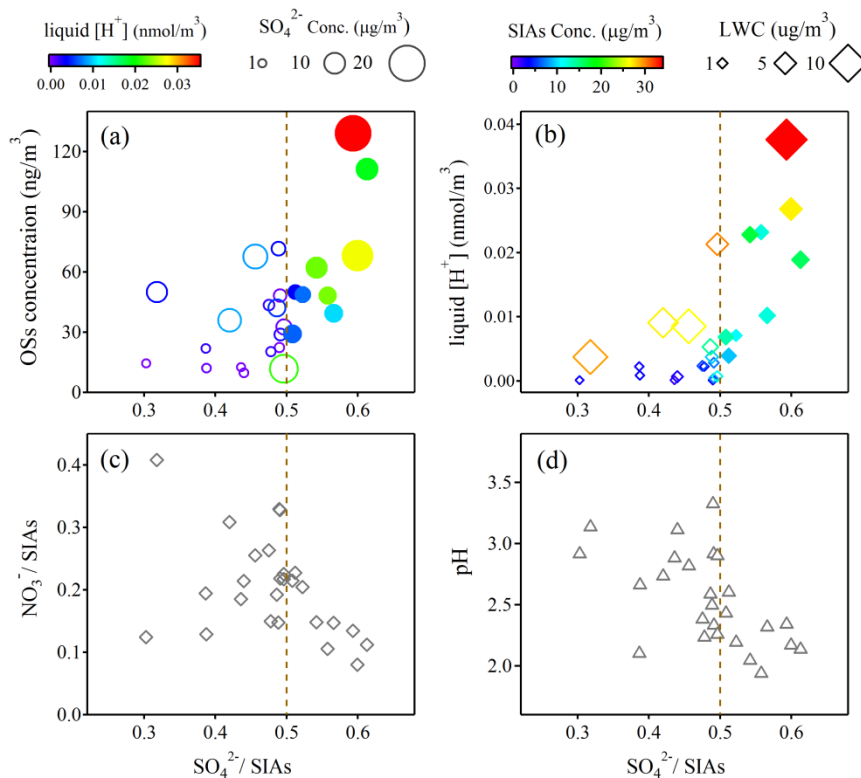
897 Figure 3 Time series of (a) wind speed (WS) and relative humidity (RH), (b) PM<sub>2.5</sub>, (c) mass concentrations of organics,  
 898 sulfate, nitrate and composition of secondary inorganic aerosols during pollution episodes (d) SO<sub>2</sub>, (e) liquid water content  
 899 (LWC) and aqueous phase [H<sup>+</sup>], and (f) the total concentrations of OSs quantified by HPLC-MS. The pollution episodes  
 900 were marked by gray shadow.

901

902

903

904



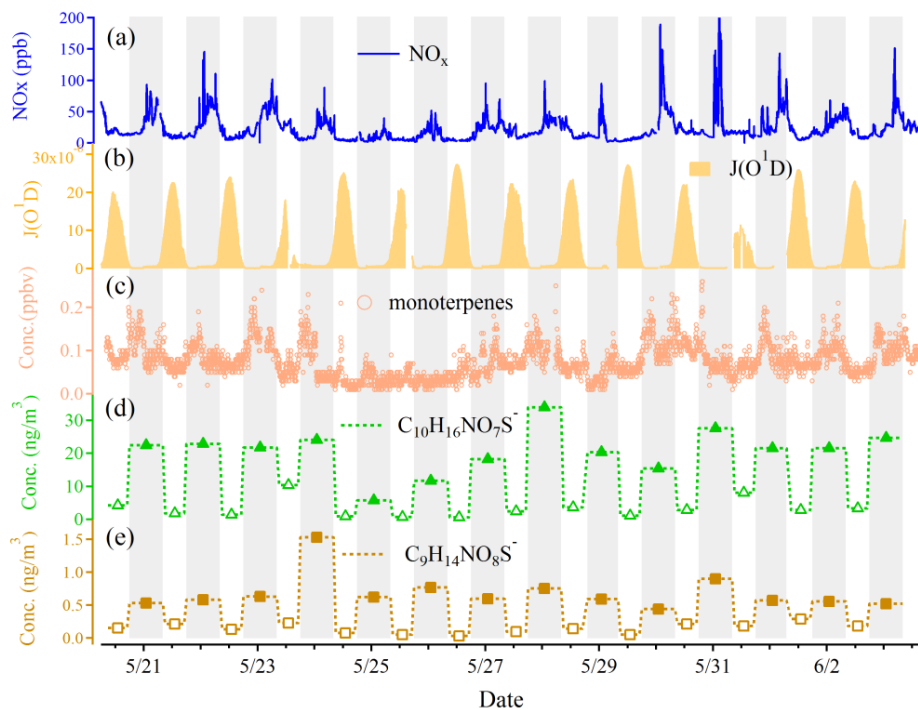
905

906 Figure 4 (a) The OS concentrations as a function of the  $\text{SO}_4^{2-}/\text{SIAs}$  mass ratios. The circles are colored according to the  
 907 liquid  $[\text{H}^+]$  concentration and the sizes of the circles are scaled to the  $\text{SO}_4^{2-}$  mass concentration. (b) The liquid  $[\text{H}^+]$  as a  
 908 function of the  $\text{SO}_4^{2-}/\text{SIAs}$  mass ratios. The markers are colored according to the SIAs mass concentrations and the sizes of  
 909 the markers are scaled to the liquid water content (LWC). (c) The  $\text{NO}_3^-/\text{SIAs}$  mass ratios as a function of the  $\text{SO}_4^{2-}/\text{SIAs}$   
 910 mass ratios. (d) The aerosol pH as a function of the  $\text{SO}_4^{2-}/\text{SIAs}$  mass ratios. The solid markers represent those among the  
 911 range  $\text{SO}_4^{2-}/\text{SIAs} > 0.5$  and hollow markers represent those among the range  $\text{SO}_4^{2-}/\text{SIAs} < 0.5$  in figure (a) and (b). When  
 912 sulfate dominated the accumulation of secondary inorganic aerosols ( $\text{SO}_4^{2-}/\text{SIAs} > 0.5$ ), both aerosol LWC and acidity ( $\text{pH} <$   
 913  $2.8$ ) increased and OS formation was obviously promoted. In comparison, the acid-catalyzed OS formation was limited by  
 914 lower aerosol acidity under nitrate-dominant conditions.

915

916

917



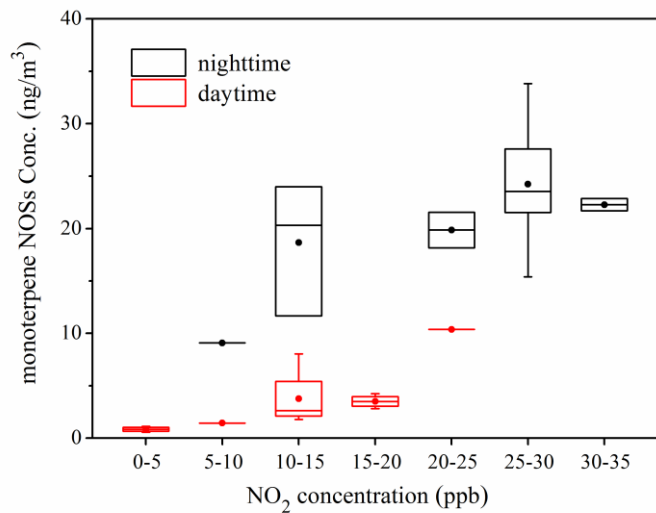
919

920 Figure 5 Time series of (a)  $\text{NO}_x$ , (b)  $J(\text{O}^1\text{D})$ , (c) monoterpene, (d) monoterpene NOSs ( $\text{C}_{10}\text{H}_{16}\text{NO}_7\text{S}$ ) and (e) limonaketone921 NOSs ( $\text{C}_9\text{H}_{14}\text{NO}_8\text{S}$ ). The gray background denotes the nighttime and white background denotes the daytime.

922

923

924

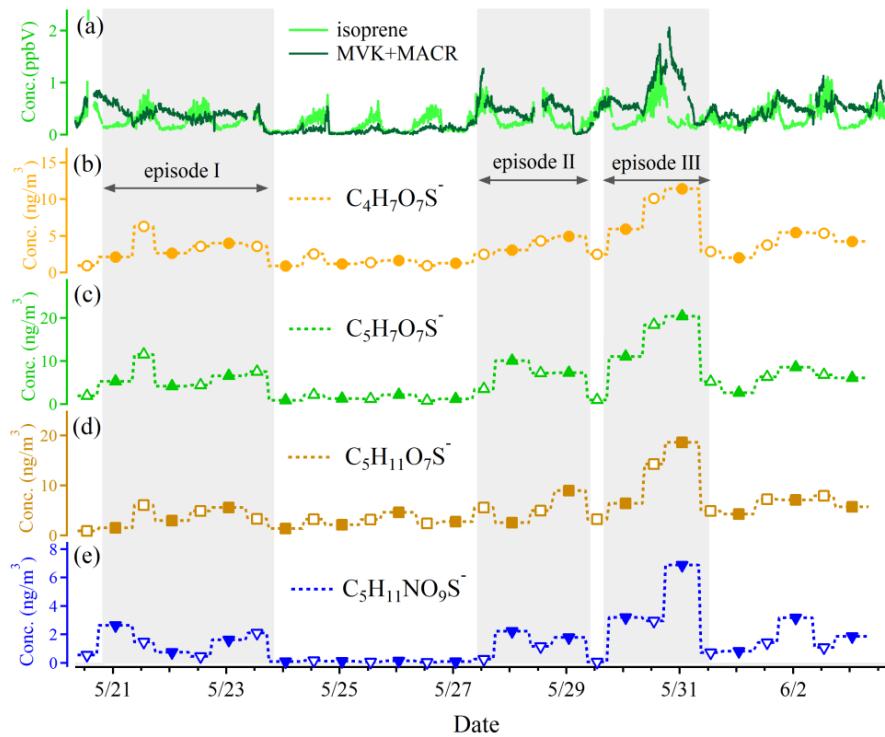


925

926 Figure 6 The concentrations of monoterpane NOSs ( $C_{10}H_{16}NO_7S^-$ ) as a function of  $NO_2$  concentration bins (ppb) during  
 927 daytime and nighttime. The closed circles represent the mean values and whiskers represent 25 and 75 percentiles.

928

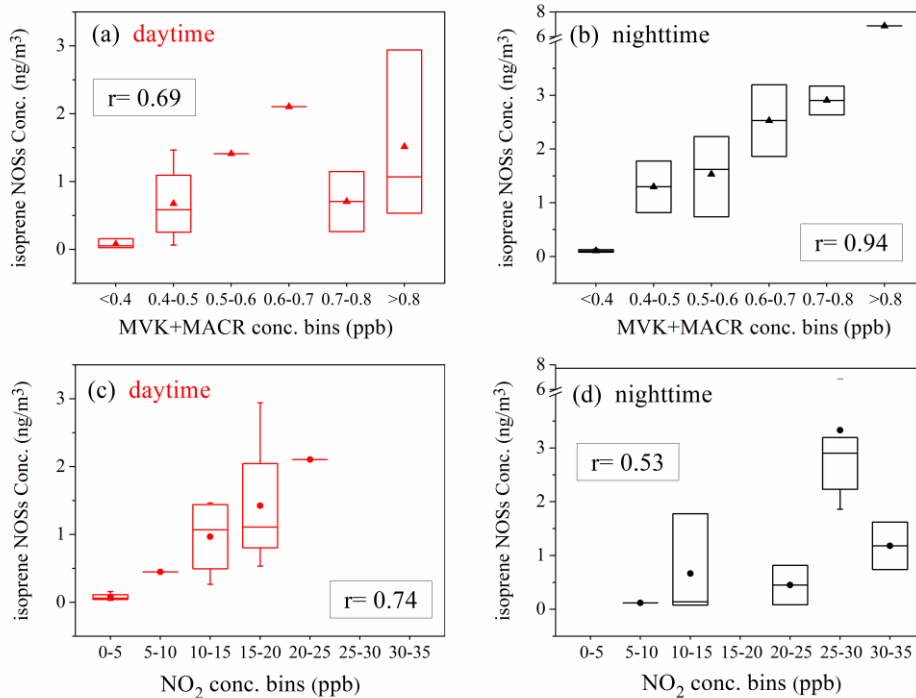
929



930

931 Figure 7 Time series of (a) isoprene and MVK+MACR, isoprene OSs (b)  $C_4H_7O_7S^-$ , (c)  $C_5H_7O_7S^-$ , (d)  $C_5H_{11}O_7S^-$  and (e)  
 932 NOSs ( $C_5H_{11}NO_9S^-$ ). The pollution episodes were marked by gray shadow. MVK and MACR are the abbreviations of  
 933 methyl vinyl ketone and methacrolein, respectively.

934



935

936 Figure 8 The isoprene NOSs ( $C_5H_{11}NO_9S^-$ ) concentrations as a function of  $NO_2$  or MVK+MACR concentration bins (ppb)

937 and the correlations between isoprene NOSs ( $C_5H_{11}NO_9S^-$ ) and  $NO_2$  or MVK+MACR. The closed markers in the box

938 represent the mean values and whiskers represent 25 and 75 percentiles in each concentration bin. The r value in each panel

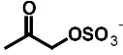
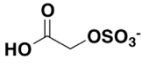
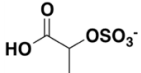
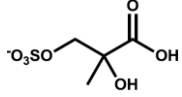
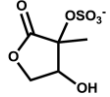
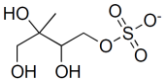
939 represents the correlation coefficient between isoprene NOSs and  $NO_2$  or MVK+MACR concentrations.

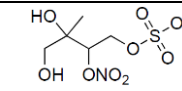
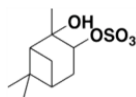
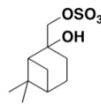
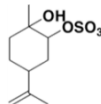
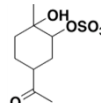
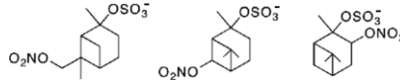
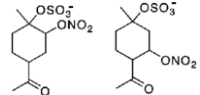
940

941

## Tables

Table 1 Organosulfates and nitrooxy-organosulfates quantified by HPLC-MS

common name	formula	[M-H] <sup>-</sup>	retention time (min)	standard	structure	concentration (ng/m <sup>3</sup> )	
						range	average (n=28)
Hydroxyacetone sulfate (HAS)	C <sub>3</sub> H <sub>5</sub> O <sub>5</sub> S <sup>-</sup>	152.99	1.7, 2.5	Glycolic acid sulfate	 (Hettiyadura et al., 2015)	0.5-7.5	2.2
Glycolic acid sulfate (GAS)	C <sub>2</sub> H <sub>3</sub> O <sub>6</sub> S <sup>-</sup>	154.97	1.6, 2.3	Glycolic acid sulfate	 (Olson et al., 2011)	3.9-58.2	19.5
Lactic acid sulfate (LAS)	C <sub>3</sub> H <sub>5</sub> O <sub>6</sub> S <sup>-</sup>	168.98	1.6, 2.6	Lactic acid sulfate	 (Olson et al., 2011)	0.7-11.9	4.4
	C <sub>4</sub> H <sub>7</sub> O <sub>7</sub> S <sup>-</sup>	198.99	1.5, 2.9	Lactic acid sulfate	 (Lin et al., 2013b; Surratt et al., 2007; Hettiyadura et al., 2015)	0.9-11.4	3.6
Isoprene OSs	C <sub>5</sub> H <sub>7</sub> O <sub>7</sub> S <sup>-</sup>	210.99	1.8, 2.9	Lactic acid sulfate	 (Surratt et al., 2008; Hettiyadura et al., 2015)	0.8-20.4	5.9
	C <sub>5</sub> H <sub>11</sub> O <sub>7</sub> S <sup>-</sup>	215.02	1.6, 2.0	Lactic acid sulfate	 (He et al., 2014; Surratt et al., 2008)	0.9-18.7	5.3

Isoprene NOS	$C_5H_{10}NO_9S^-$	260.01	4.9	Lactic acid sulfate	 (Surratt et al., 2007)	0.03-6.9	1.4
$\alpha$ -pinene OS	$C_{10}H_{17}O_5S^-$	249.08	22.7	$\alpha$ -pinene OS	 (Wang et al., 2017d; Surratt et al., 2008)	0.01-0.5	0.06
$\beta$ -pinene OS	$C_{10}H_{17}O_5S^-$	249.08	22.4, 23.4	$\beta$ -pinene OS	 (Wang et al., 2017d; Surratt et al., 2008)	0.07-0.8	0.4
Limonene OS	$C_{10}H_{17}O_5S^-$	249.08	21.8, 23.8	Limonene OS	 (Wang et al., 2017d)	0.01-0.1	0.05
Limonaketone OS	$C_9H_{15}O_6S^-$	251.06	14.0	Limonaketone OS	 (Wang et al., 2017d)	0.00-0.2	0.06
Monoterpene NOSs	$C_{10}H_{16}NO_7S^-$	294.06	24.8, 26.6, 27.1	$\alpha$ -pinene OSs	 (Surratt et al., 2008; He et al., 2014)	0.6-33.8	12.0
	$C_9H_{14}NO_8S^-$	296.04	21.1	Limonaketone OS	 (Surratt et al., 2008)	0.03-1.5	0.4